# Mechanochemical synthesis and investigation of nanomaterials for lithium-ion batteries


## N.V. Kosova

*Institute of Solid State Chemistry and Mechanochemistry SB RAS, Novosibirsk, Russia*



MolE 2012

Dubna, August 27-30

# Outline

- Intercalation electrode materials for lithium-ion batteries. Challenge for nanosized materials
- Mechanical activation as a promising method to prepare nanomaterials. Synthetic reactions
- Investigation of as prepared materials. Some examples
- Composite cathode materials

# Structural types of cathode materials

## Spinel (3D)

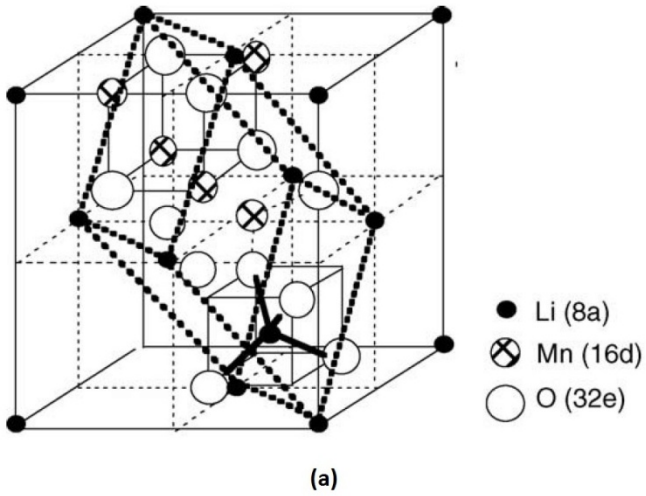


## Layered (2D)

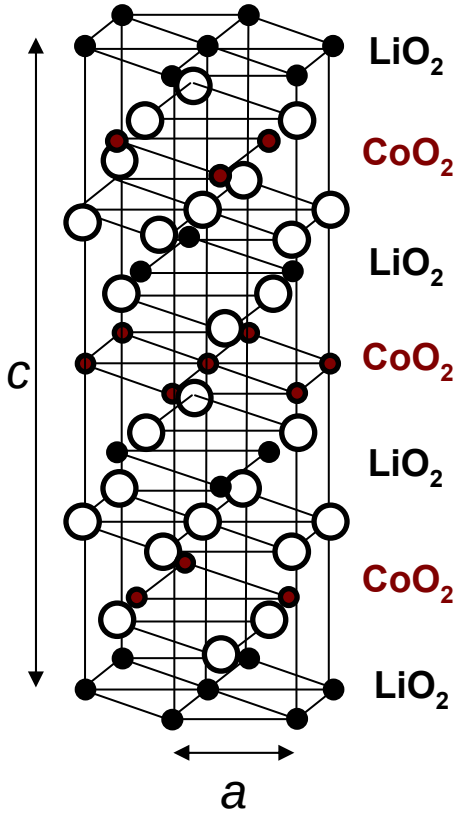


## Frame-work (1D)

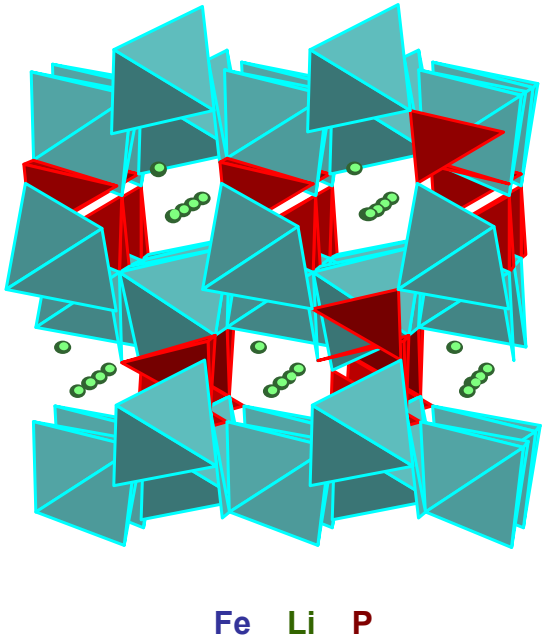

# Comparison of cathode materials

| Compound/ property | Electric conductivity | Structural, chemical and thermal stability | Complexity of synthesis |
|---|---|---|---|
| $LiCoO_2$ | 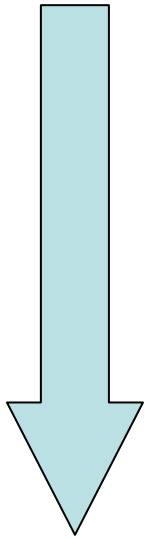 decreases | 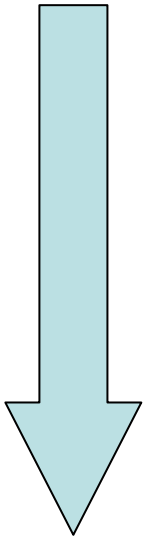 increases | 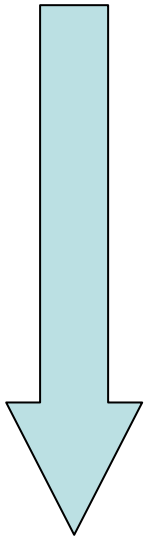 increases |
| $LiMn_2O_4$ | | | |
| $LiFePO_4$ | | | |

# Materials prepared via mechanochemical route

## Layered structured

- $LiCoO_2$
- $LiCo_{1-x}M_xO_2$
- $LiCoO_2$-$Li_2MnO_3$
- $LiNiO_2$
- $LiNi_{1-x}Co_xO_2$
- $LiNi_{1-x-y}Co_xMn_yO_2$
- $LiV_3O_8$

## Spinel structured

- $LiMn_2O_4$
- $LiMn_{2-x}M_xO_4$
- $LiMn_{1.5}Ni_{0.5}O_4$ (5V)
- $Li_4Ti_5O_{12}$ (anode)

## Frame-work structured

- $LiFePO_4$
- $LiFe_{1-x}Mn_xPO_4$
- $LiMnPO_4$
- $LiCoPO_4$
- $LiNiPO_4$
- $Li_2CoPO_4F$
- $Li_2NiPO_4F$
- $LiVPO_4F$
- $Li_2FeP_2O_7$
- $LiTi_2(PO_4)_3$ (electrolyte)

# Pros and cons of nanosized electrode materials

The particle size (and its distribution), morphology and density of the particles play a fundamental role on electrochemical performance of electrode materials

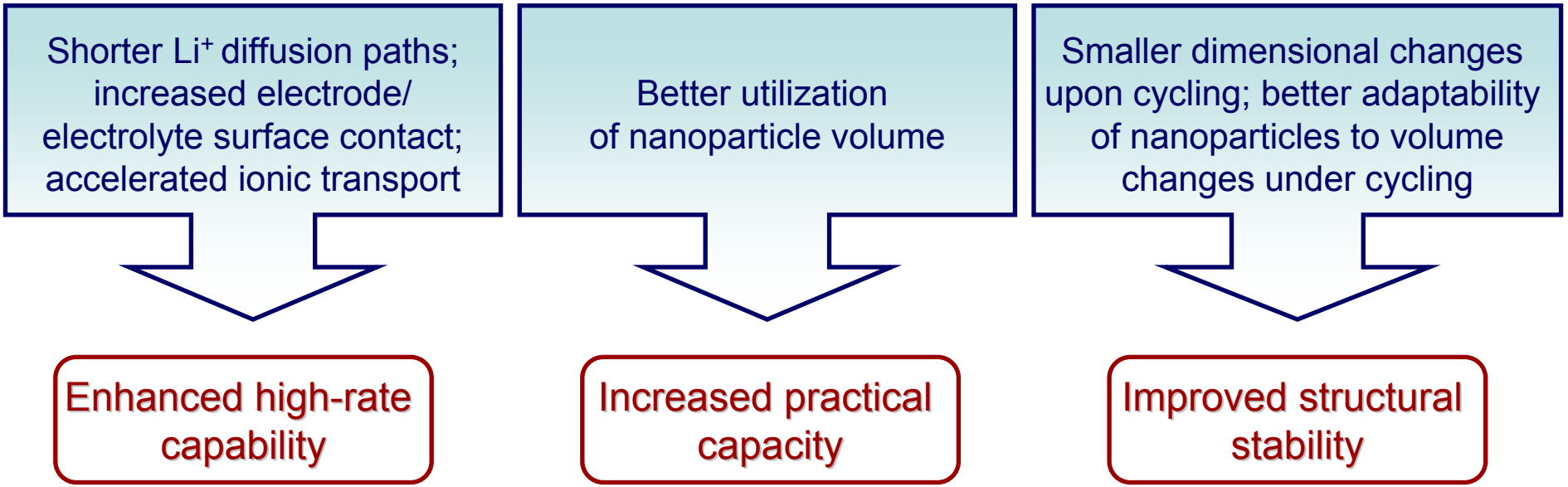


☹ Intensification of undesirable electrode/electrolyte reactions due to high surface area (self-discharge, poor cycling and calendar life)

☹ Inferior packing of particles (low volumetric energy densities)

☹ Potentially more complex synthesis

# Mechanical activation method
# Synthetic reactions

# Nanomaterials via mechanical activation

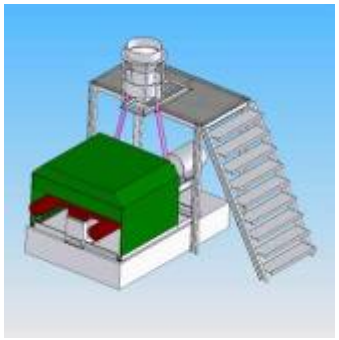

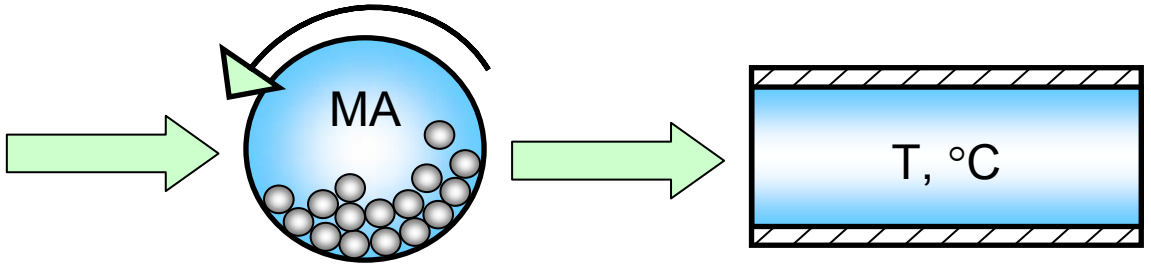


**Two-step process:**

**1 step** (MA) – grinding and plastic deformation of solids → mixing of components at molecular level (deformation mixing);

**2 step** (T) – short-time thermal treatment → formation of product from molecular precursor supersaturated by defects

Laboratory planetary mill AGO-2

☺ Decrease in a number of intermediate stages
☺ Acceleration and simplification of the synthetic process
☺ Increase in homogeneity of the final product
☺ Formation of nano-sized / nano-structured material

Industrial activator CEM-7

# Synthetic reactions

- Soft mechanochemical synthesis (SMS)
- Mechanochemically assisted carbothermal reduction of *d*-metal compounds (CTR)
- Mechanochemically assisted interaction of covalent compounds with ionic salts

Motivation - to realize fast propagating synthesis in order to reduce contamination and energy consumption and to prepare nanosized products.

# 1. Soft mechanochemical synthesis (SMS)

SMS is generally based on the acid-base properties of the reagents.

$$A(OH)_x + B(OH)_y \xrightarrow{MA} AB(OH)_m \cdot nH_2O \xrightarrow{T} ABO_z$$

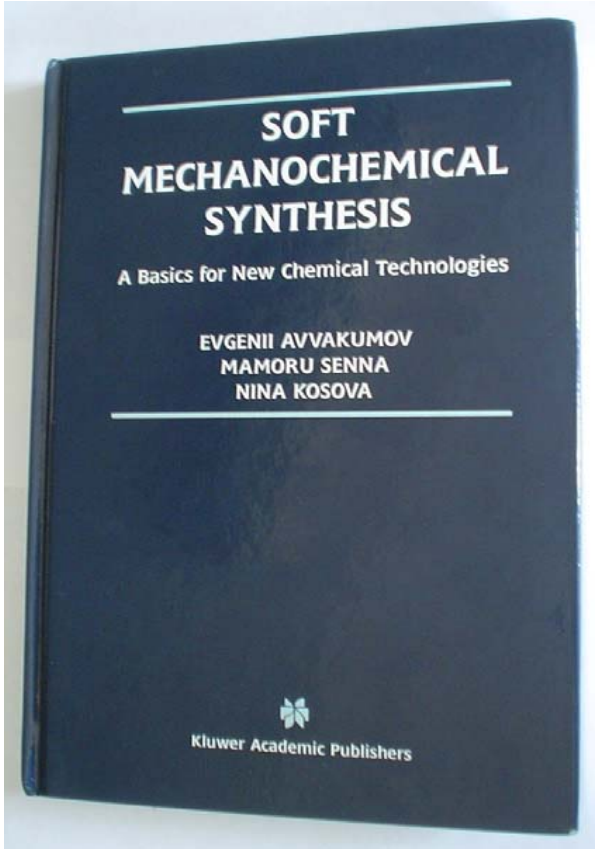


1. Acceleration of initial interaction due to participation of OH groups in the processes of proton and electron transfer.

2. Formation of chemically active X-ray amorphous precursor.

3. Formation of final product by heating the precursor at moderate temperatures.

4. Significant reduction of contamination due to lower hardness of initial reagents.

5. Preparation of nanosized, pure and homogeneous final product as a result.

# SMS: $LiMn_2O_4$

**$LiOH + MnO_x \rightarrow LiMn_2O_4$**

$MnO \rightarrow Mn_2O_3 \rightarrow MnO_2$ acidity increases

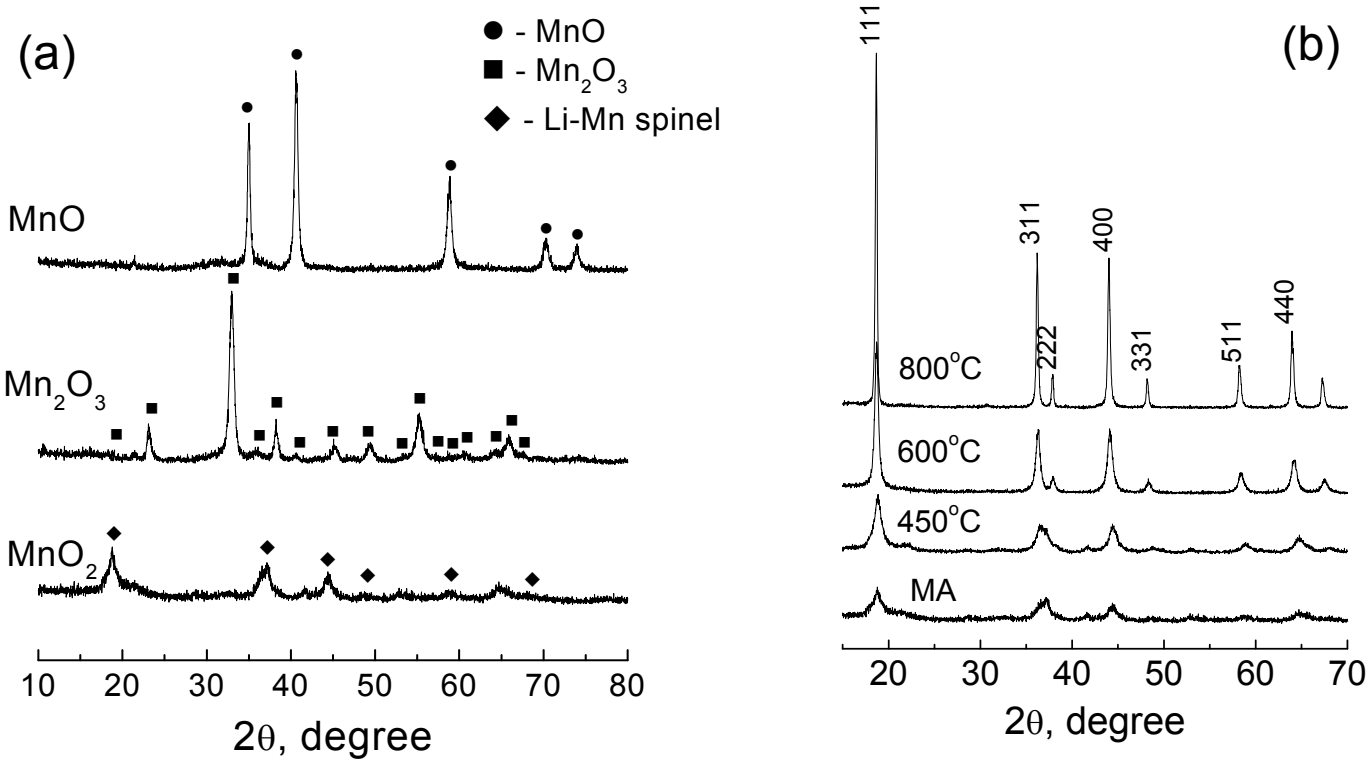


X-Ray patterns of (a) mechanically activated mixtures of LiOH with different Mn oxides and (b) the products of MA and annealing at different temperatures.

**SMS - fast propagating mechanochemical reaction (realized at the stage of MA)**


N.V. Kosova et al., Solid State Ionics 135 (2000) 107-114.
N.V. Kosova et al., J. Power Sources 97-98 (2001) 406-411.

# SMS: $LiV_3O_8$

**$2LiOH + 3V_2O_5 \rightarrow 2LiV_3O_8 + H_2O$**

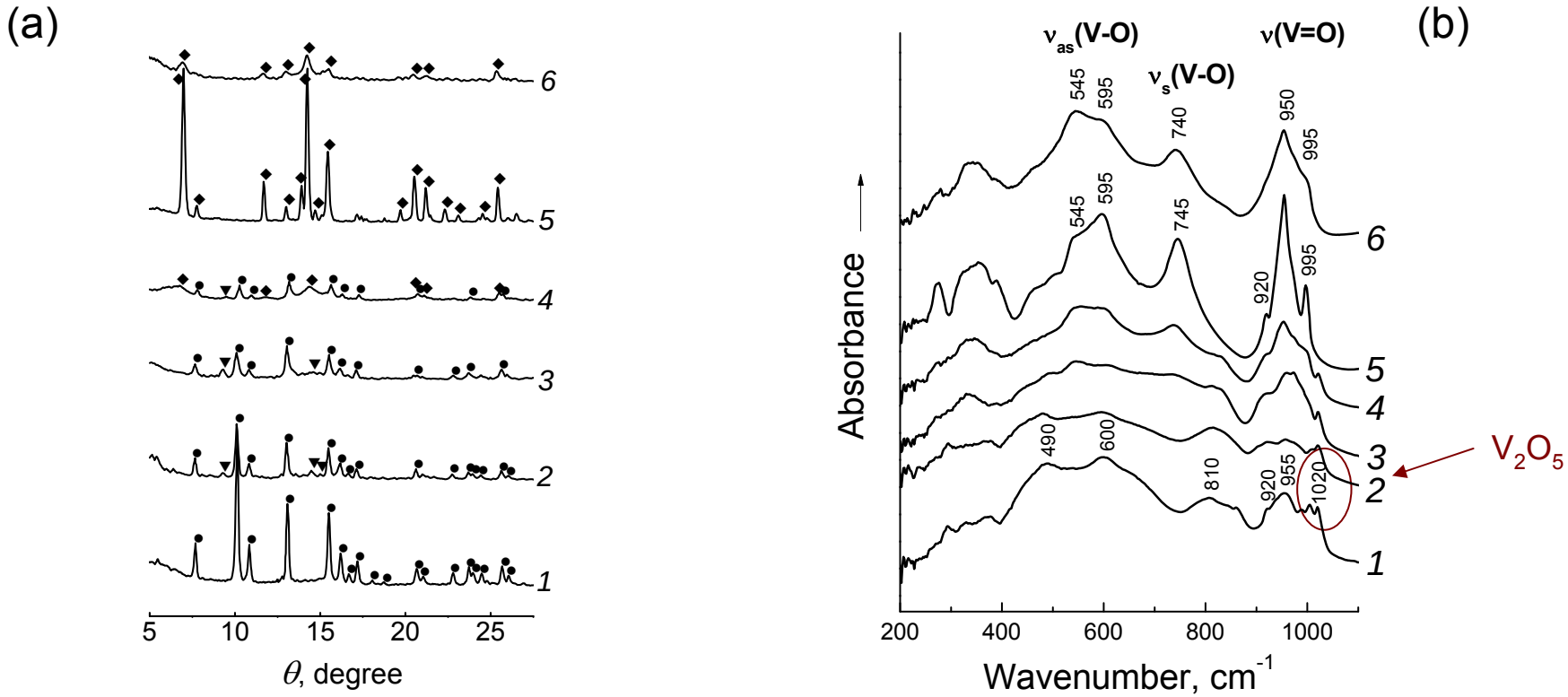


X-ray patterns (a) and FTIR spectra (b) of the $LiOH+V_2O_5$ mixtures activated for *(1)* 30 sec, *(2)* 1 min, *(3)* 5 min, *(4)* 10 min, *(5)* 10 min followed by annealing at 400°C, *(6)* 5 min followed by aging for 6 months.

● $V_2O_5$; ♦ $LiV_3O_8$; ▼ Li-V bronzes



N.V. Kosova et al., J. Solid State Chem. 160 (2001) 444-449.

# 2. Carbothermal reduction

The potential low-cost advantage of $LiFePO_4$ is not realized if expensive $Fe^{2+}$ precursors are used as reagents.

**Carbothermal reduction method** is relied on the use of carbon both as a selective reducing and covering agent (J. Barker, 2003) :

1) $Fe^{3+}$ compounds are cheaper than $Fe^{2+}$ salts;

2) less hazardous gases are formed during firing;

3) more easy to scale-up.

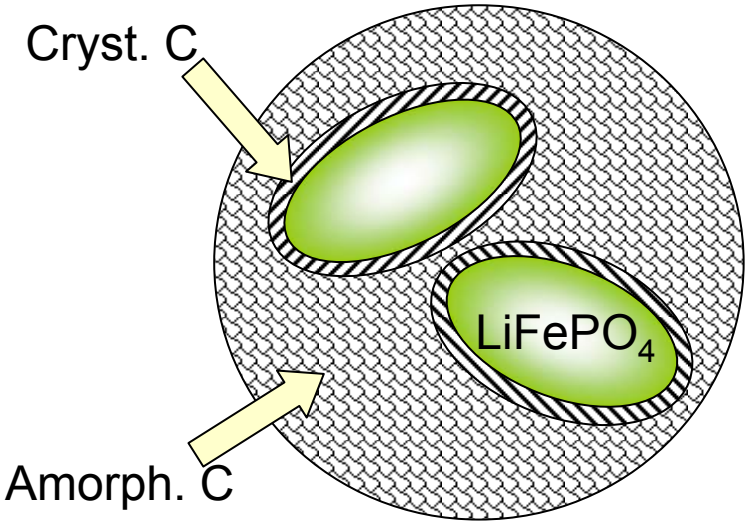


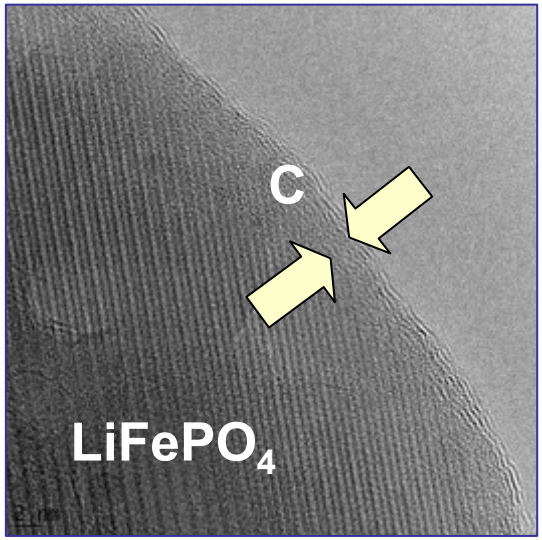

# Mechanochemically assisted CTR of $Fe_2O_3$

$$Li_2CO_3 + \mathbf{Fe_2O_3 + C} + 2(NH_4)_2HPO_4 \rightarrow 2LiFePO_4 + 3H_2O + 4NH_3 + CO_2 + CO$$

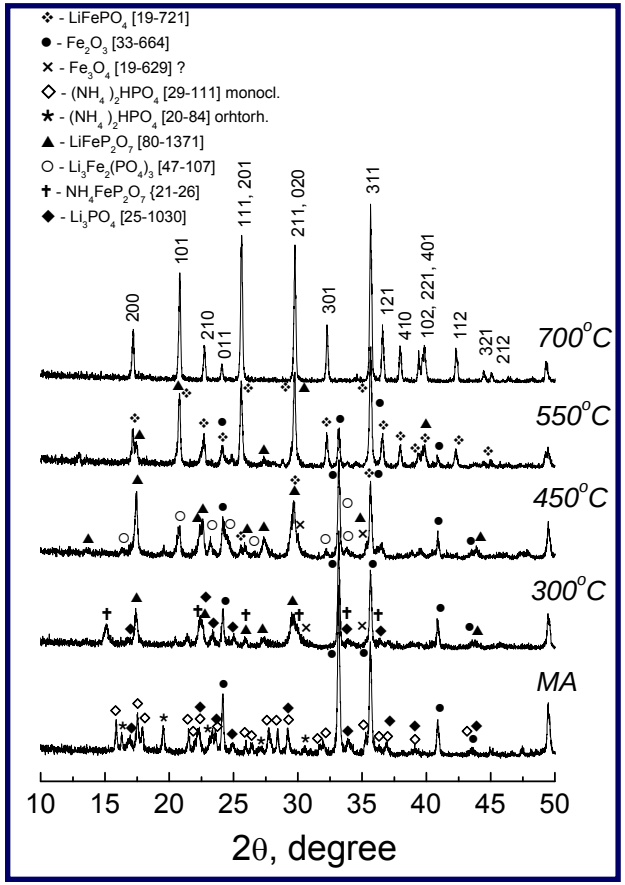


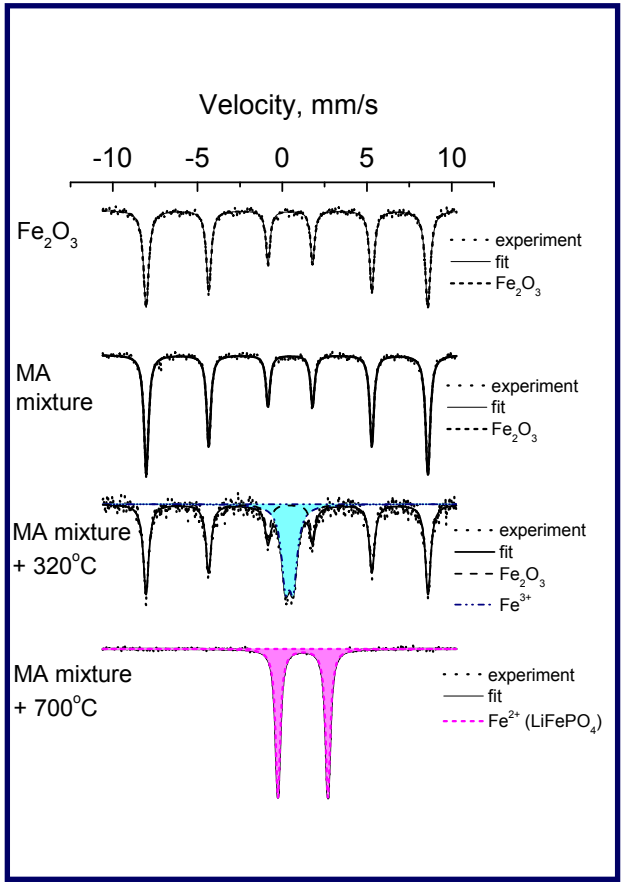


X-Ray patterns and Mössbauer spectra of the activated and annealed mixtures with $Fe_2O_3$.



N.V. Kosova et al., J. Electrochem. Soc. 157 (2010) A1247-A1252.

# Carbothermal reduction: $LiMPO_4$ (M=Mn, Fe, Co)

$$Li_2CO_3 + \mathbf{2MnO_2 + 2C} + 2(NH_4)_2HPO_4 \rightarrow 2LiMnPO_4 + 3H_2O + 4NH_3 + CO_2 + 2CO$$

$$Li_2CO_3 + \mathbf{Fe_2O_3 + C} + 2(NH_4)_2HPO_4 \rightarrow 2LiFePO_4 + 3H_2O + 4NH_3 + CO_2 + CO$$

$$3Li_2CO_3 + \mathbf{2Co_3O_4 + C} + 6(NH_4)_2HPO_4 \rightarrow 6LiCoPO_4 + 12H_2O + 12NH_3 + 3CO_2 + CO$$

---

$$Li_2CO_3 + \mathbf{2NiO} + 2(NH_4)_2HPO_4 \rightarrow 2LiNiPO_4 + 3H_2O + 4NH_3 + CO_2$$

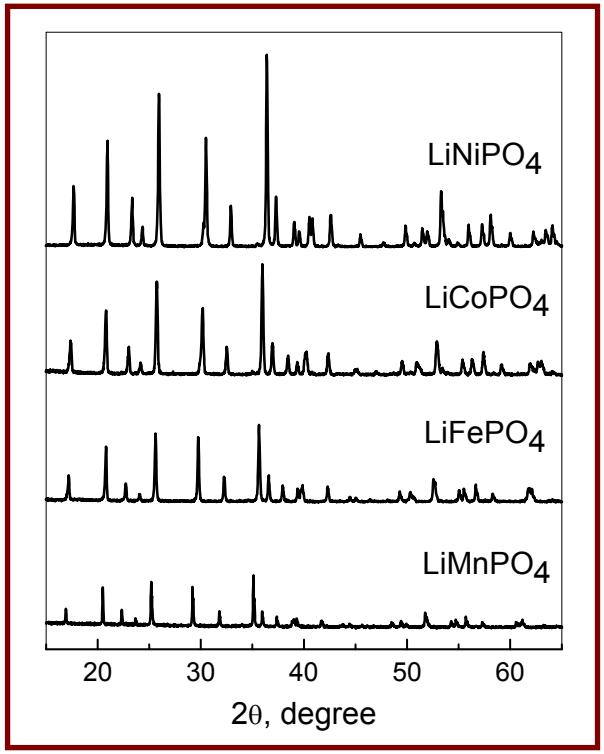

# 3. Covalent + ionic salts

This approach, called ***"dimensional reduction"***, was first outlined by Long et al. It involves a deconstruction of the bonding within a covalent metal – anion framework by reaction with an ionic reagent, to provide a less tightly connected framework that retains the metal coordination geometry and polyhedron connectivity of the parent structure (**$Li_2CoPO_4F$** and **$Li_2NiPO_4F$**). On the other hand, the formation of **$LiVPO_4F$** by incorporating of LiF into the framework of $VPO_4$ (S.g. Cmcm) represents a decrease in crystal symmetry, but here, a three-dimentional framework is maintained.

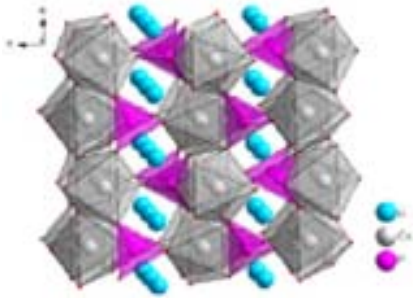

$LiCoPO_4$
(corner-shared $CO_6$)

- **$LiCoPO_4 + LiF \rightarrow Li_2CoPO_4F$**
- **$LiNiPO_4 + LiF \rightarrow Li_2NiPO_4F$**
- **$VPO_4 + LiF \rightarrow LiVPO_4F$**

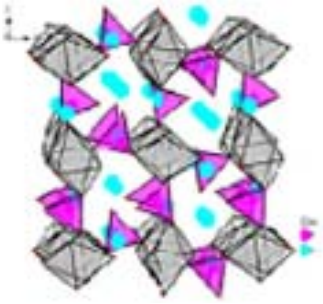

$Li_2CoPO_4F$
(edge-shared $CoO_4F_2$)

J.R. Long, L.S. McCarty, R.H. Holm, J. Am. Chem. Soc. 118 (1996) 4603.

# Covalent + ionic salts

D8 Advance Bruker diffractometer, HTK 1200N temperature-controlled X-ray chamber.

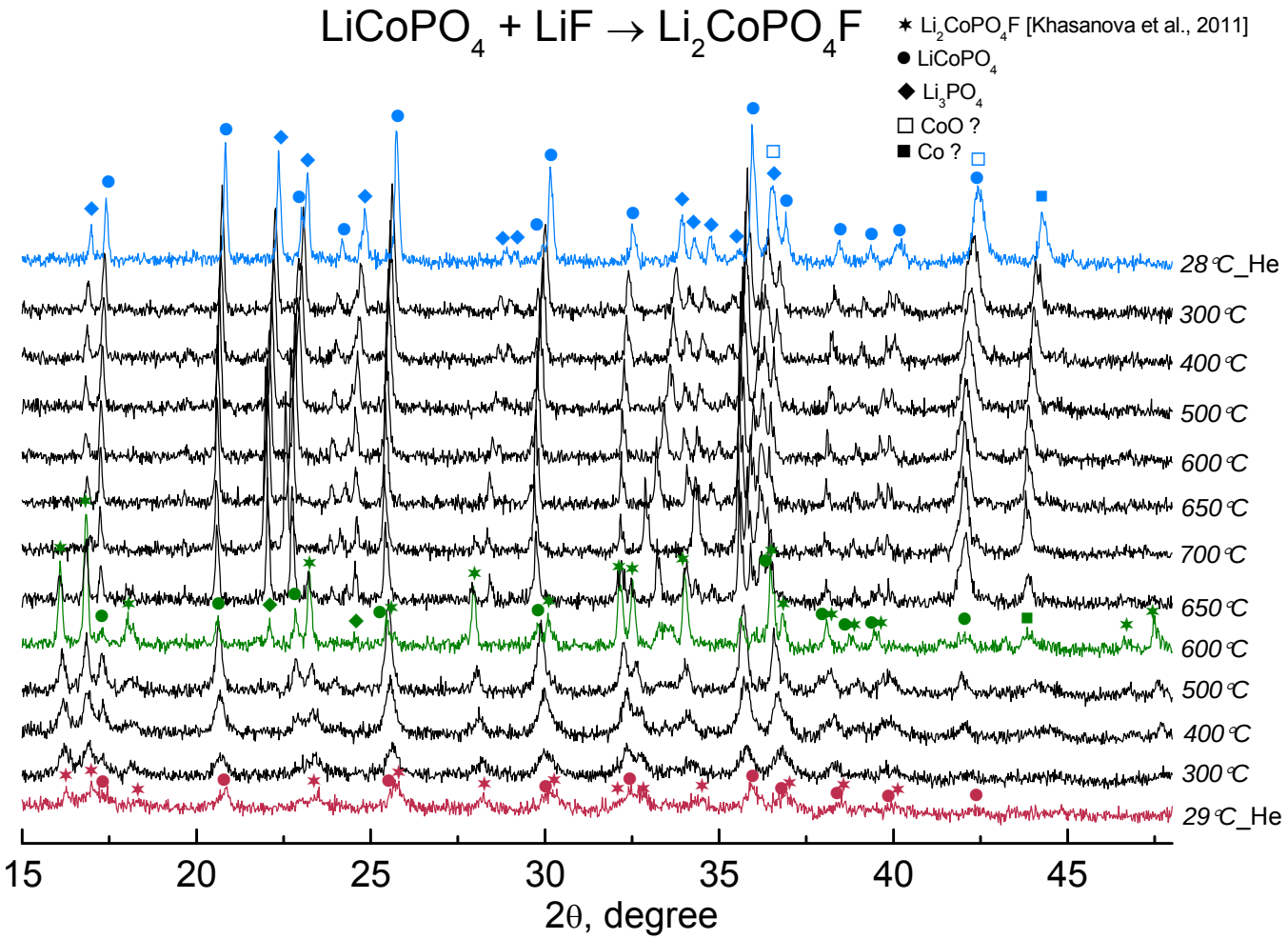


Phase transformation under heating and cooling of the activated mixture.

**Fast propagating mechanochemical reaction (realized at the stage of MA)**



N.V. Kosova et al., Solid State Ionics doi:10.1016/j.ssi.2011.11.007

# Investigation of as prepared materials

# Investigation methods

| Particle size and morphology | Crystal and local structure | Electronic structure | Electrochemical properties |
|---|---|---|---|

- X-ray powder diffraction (XRD)
- Thermal analysis (DTA and TG)
- Infrared spectroscopy (FTIR)
- Raman spectroscopy (RS)
- Mössbauer spectroscopy
- Nuclear magnetic resonance spectroscopy (NMR)
- Electron paramagnetic resonance spectroscopy (EPR)
- X-ray photoelectron spectroscopy (XPS)
- Scanning electron microscopy (SEM)
- Transmission electron microscopy (TEM)
- Galvanostatic cycling
- Impedance spectroscopy
- *In situ* synchrotron diffraction

# Li - Mn spinels

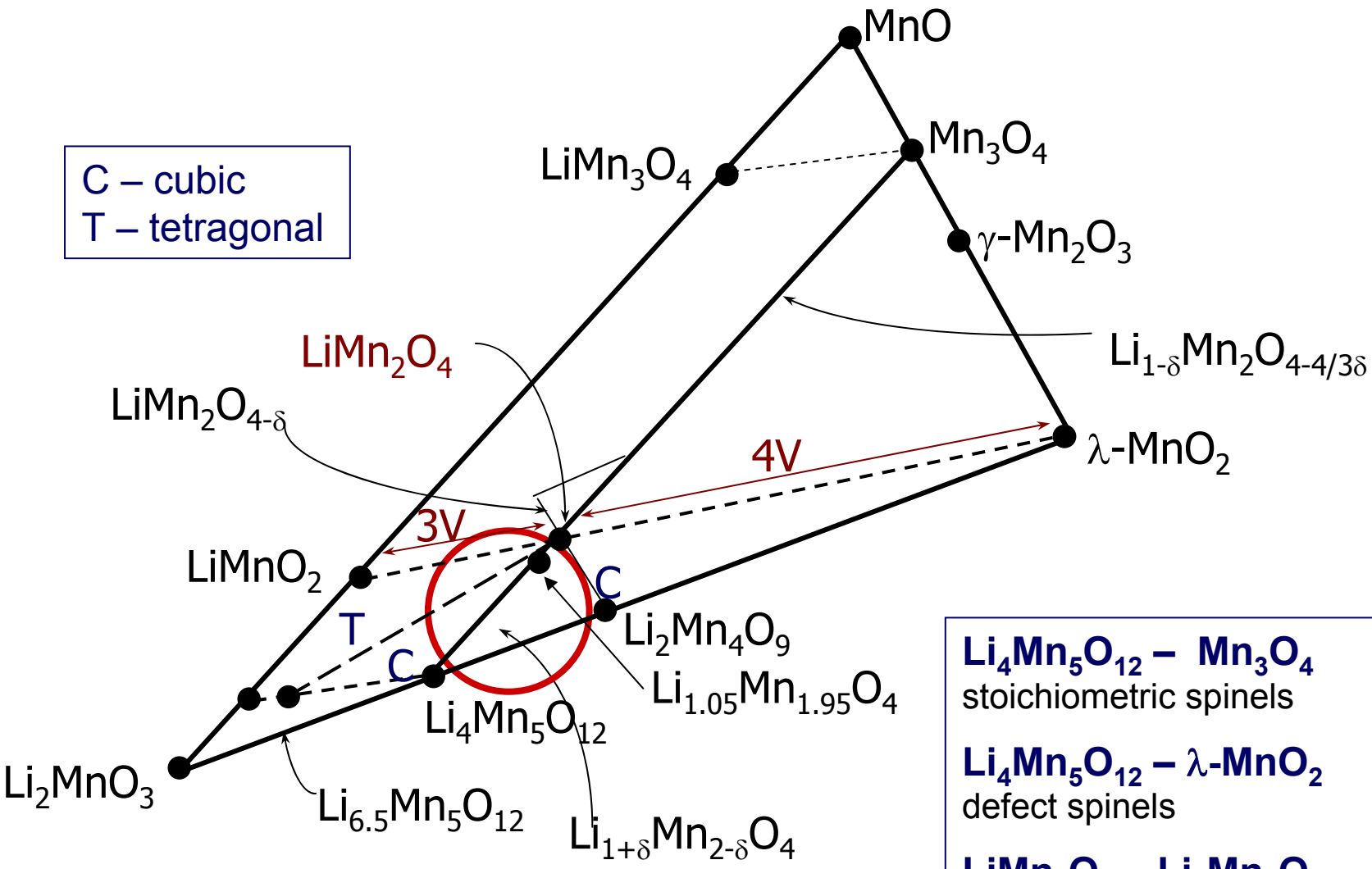


**$Li_4Mn_5O_{12}$ – $Mn_3O_4$**
stoichiometric spinels

**$Li_4Mn_5O_{12}$ – $\lambda$-$MnO_2$**
defect spinels

**$LiMn_2O_4$ – $Li_2Mn_4O_9$**
oxygen non-stoichiometric spinels

M. Thackerey et al., 1992

# Cycling of micronsized $LiMn^{3+}Mn^{4+}O_4$

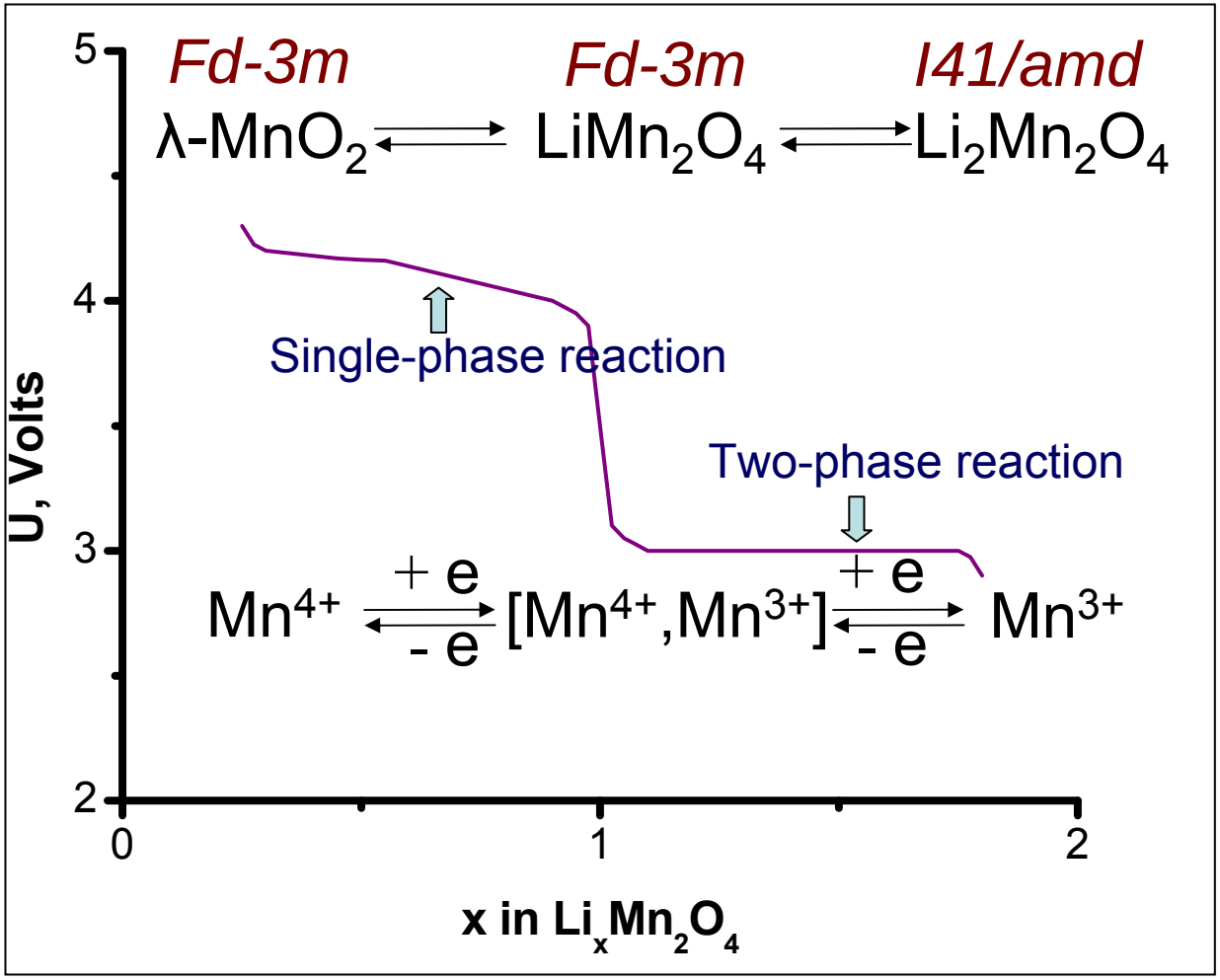


Jan-Teller distortion

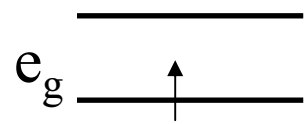


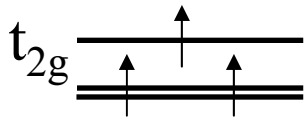


$Mn^{3+}$ $(d^4)$

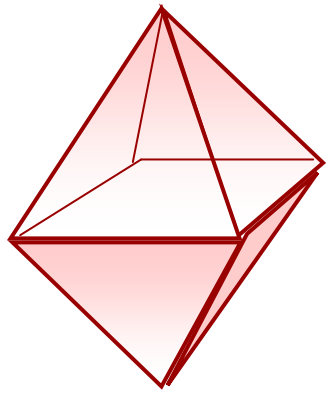

$\Delta V/V$ = 10 - 16%

# Cycling of nanosized $LiMn_2O_4$

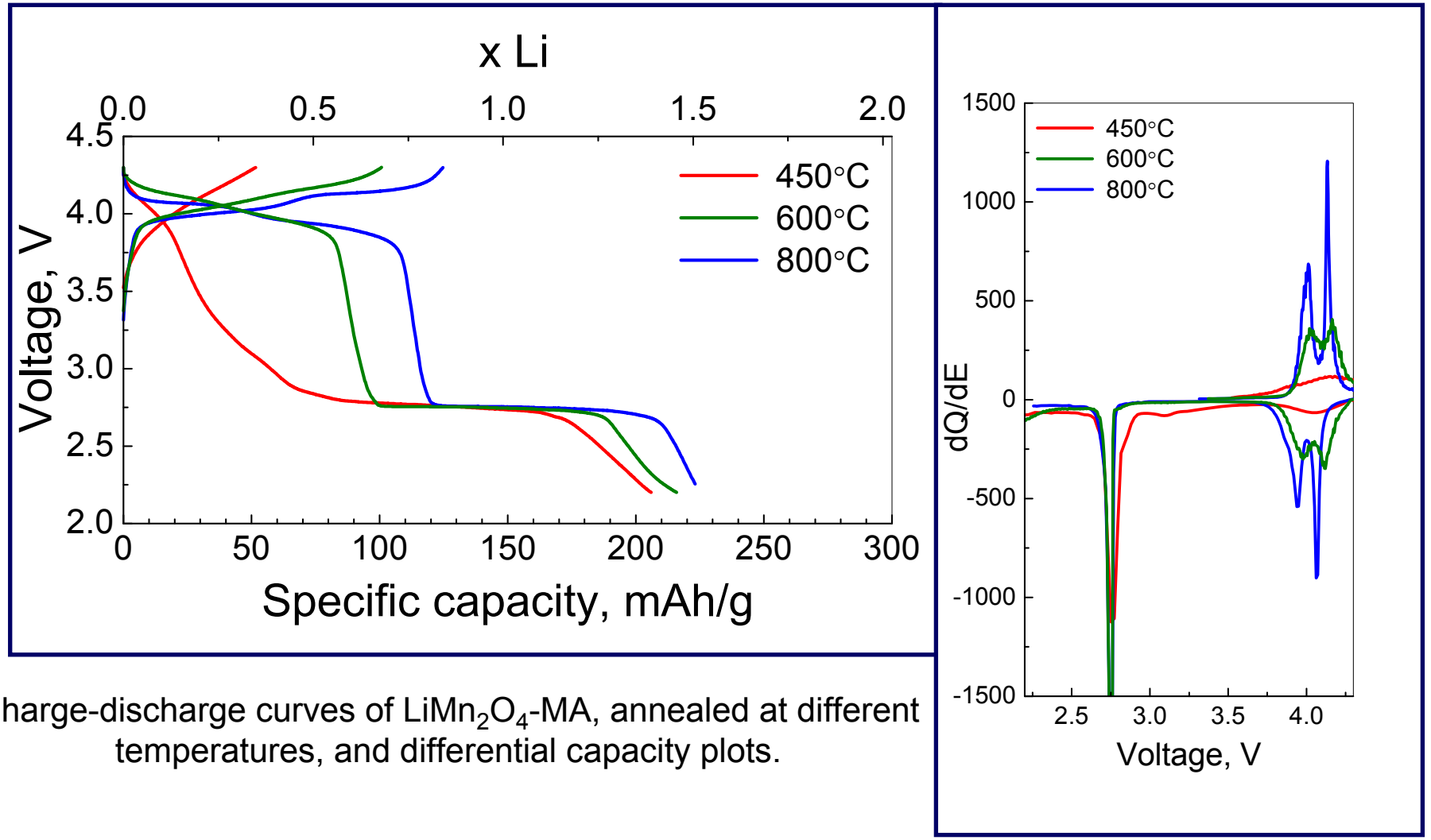


Charge-discharge curves of $LiMn_2O_4$-MA, annealed at different temperatures, and differential capacity plots.

Nano-spinel cannot accommodate domain boundaries between Li-rich and Li-poor phases due to interface energy, and therefore lithiation proceeds via solid solutions without domain boundaries, enabling fast Li-ion insertion.



N.V. Kosova, E.T. Devyatkina, Russ. J. of Electrochem. 48 (2012) 320-329.

# $LiNi_{0.5}Mn_{1.5}O_4$: structure and properties

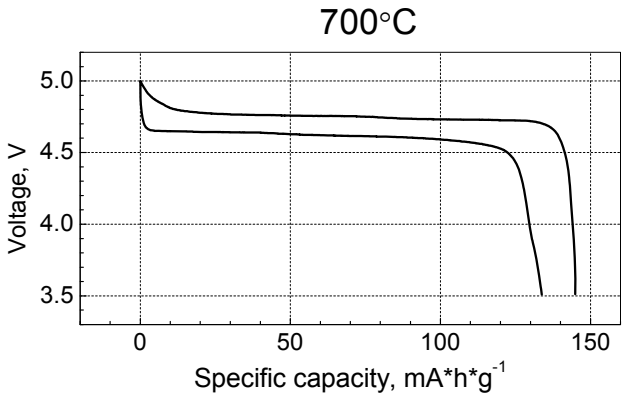


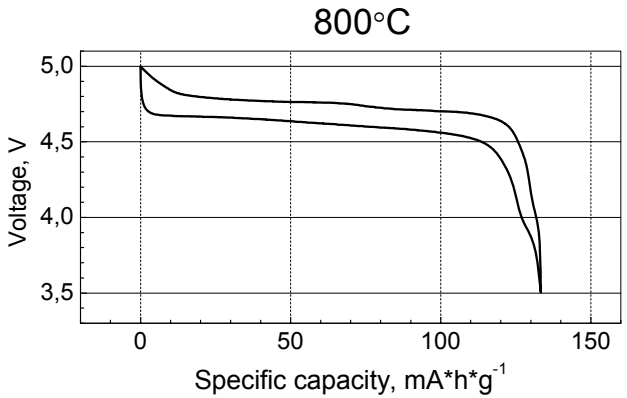


$P4_332$

Fd3m

5 V cathode material:

$Ni^{2+}$ two-electron reaction

$Mn^{4+}$ electrochemically non-reactive

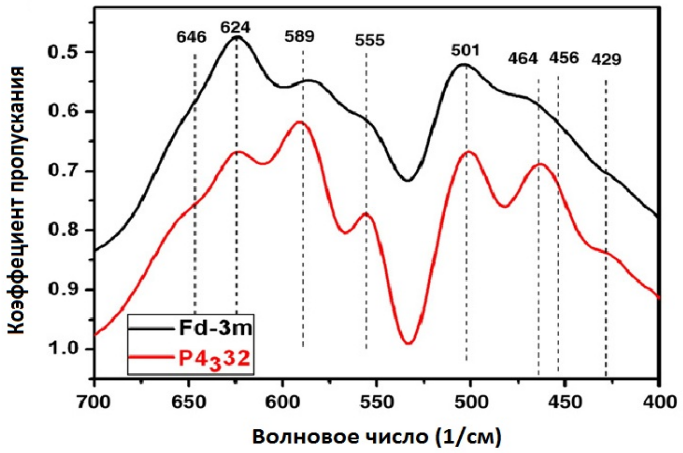




N.V. Kosova et al., 16 IMLB, Jeju, Korea, June 17-22, 2012.

# Synthesis of layered $LiNi_{0.8}Co_{0.2}O_2$

From double hydroxides

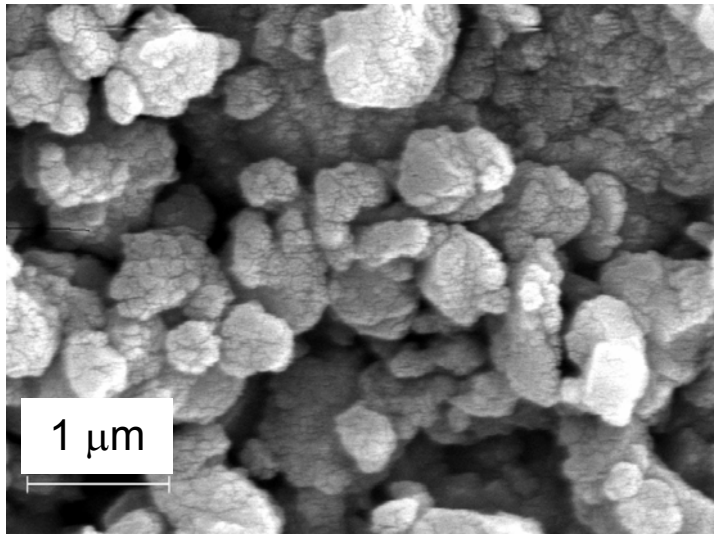


$LiOH + (Ni_{0.8}Co_{0.2})(OH)_2$

From anhydrous oxides

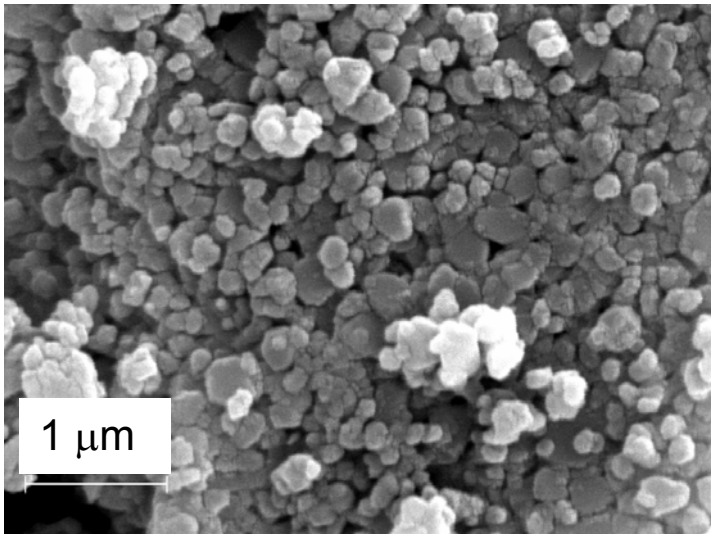


$LiOH + NiO + Co_3O_4$

N.V. Kosova et al., Chemistry for Sustainable Development 17 (2009) 141-149.

# $LiNi_{1-y}Co_yO_2$: local structure and electrochemistry

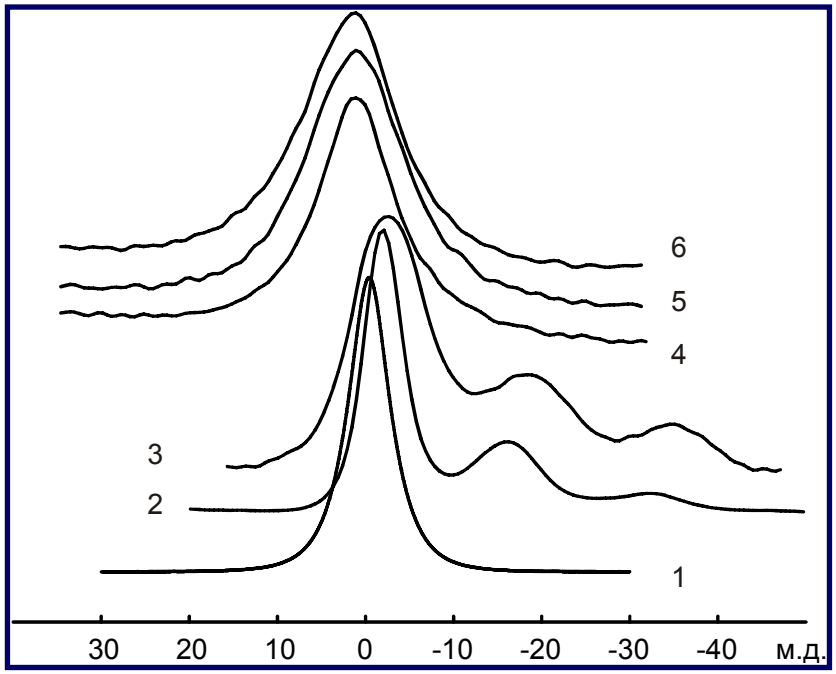


$^7Li$ MAS NMR spectra of $LiNi_{1-y}Co_yO_2$: y = 1 (1); y = 0.8 (2); y = 0.6 (3); y = 0.4 (4); y = 0.2 (5); y = 0 (6).

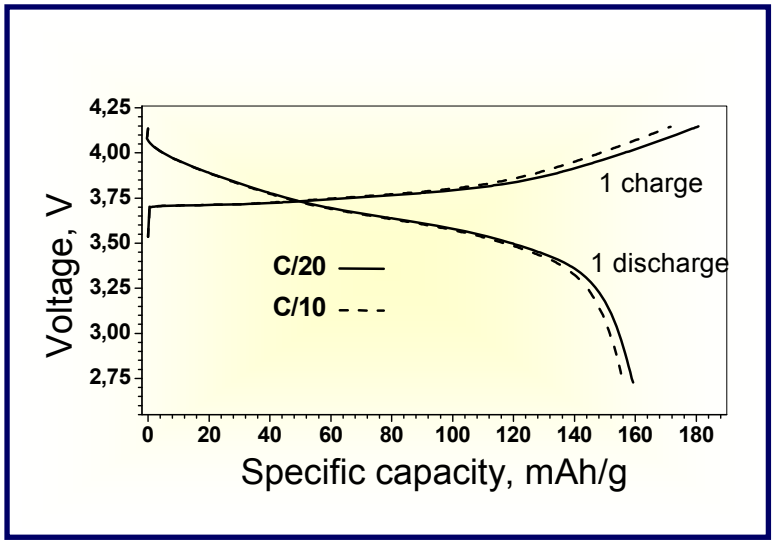


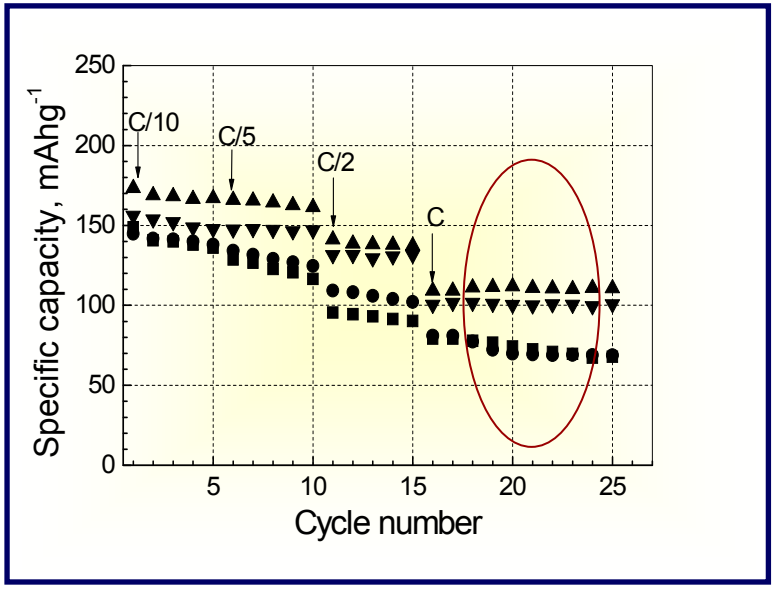


▲ y = 0,2; ▼ 0,4; ● 0,6; ■ 0,8

# $LiFePO_4$: effect of nano-sizing and surface disordering

Prepared from $FeC_2O_4$

450°C

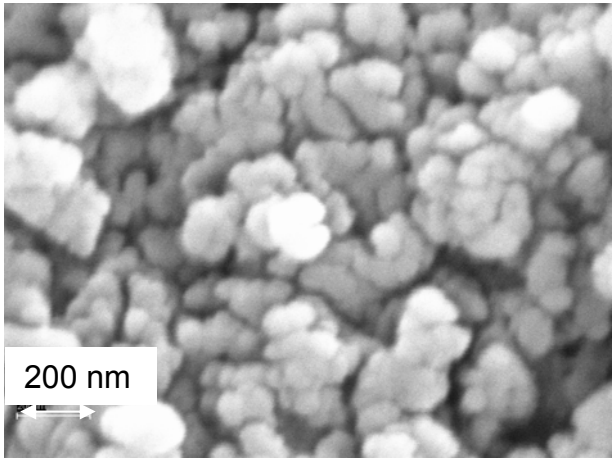


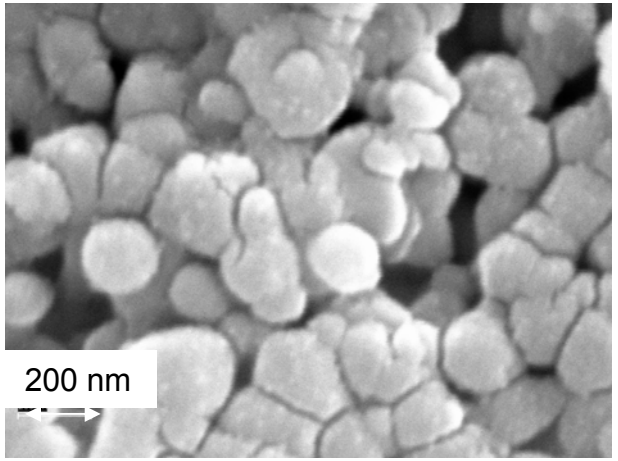


700°C

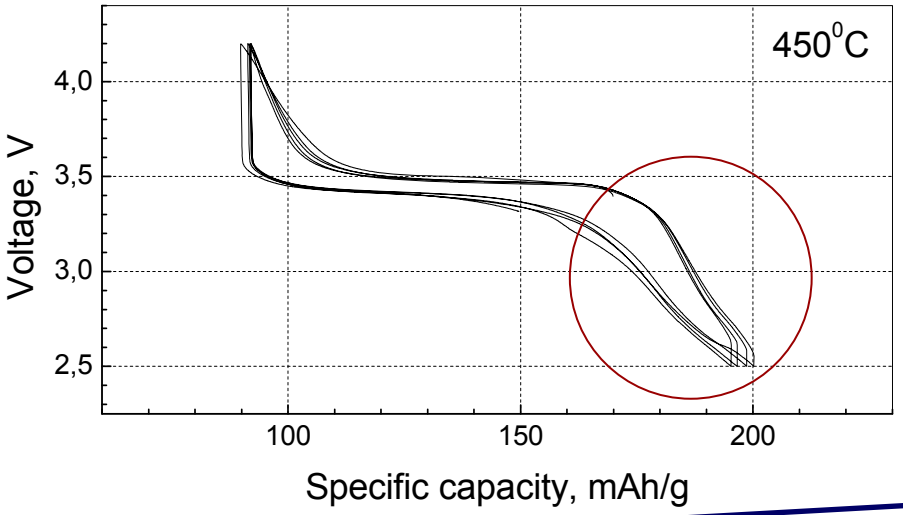


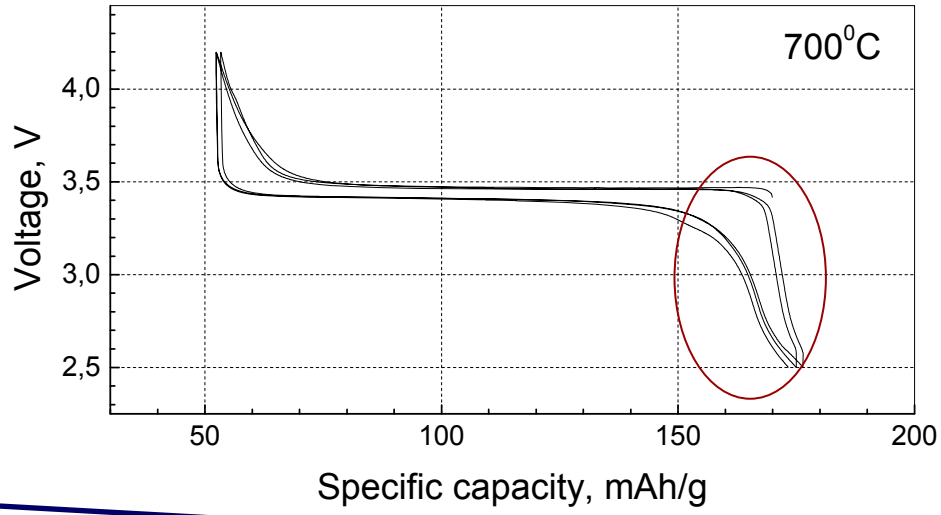


Increased ranges of solid solution formation, decreased miscibility gap



N.V. Kosova et al., J. Electrochem. Soc. 157 (2010) A1247-A1252.

# Mechanism of Li deintercalation in nano-sized $LiFePO_4$

Micro-particles

Nano-particles

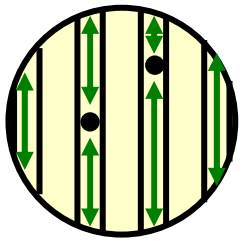

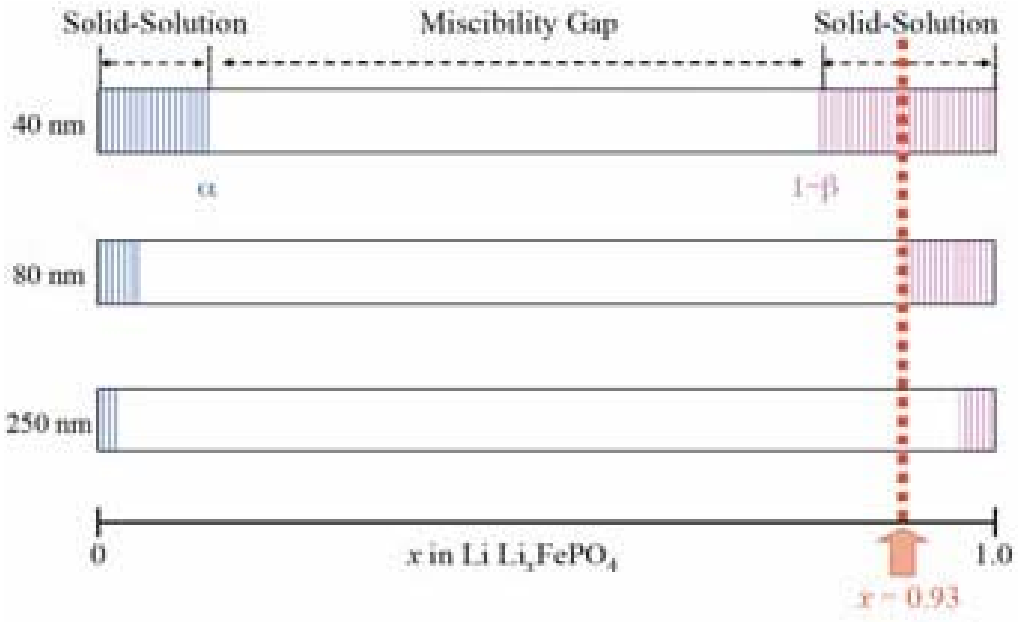


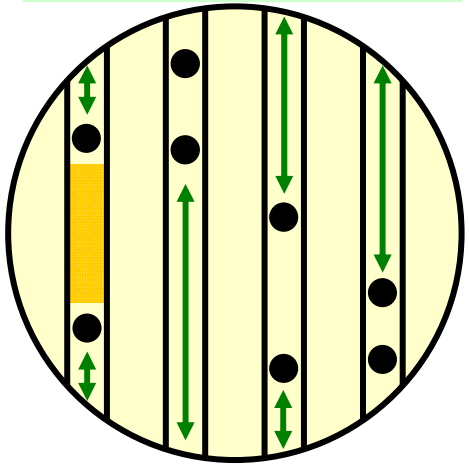

Full capacity at high rates

Capacity is partially lost

Two-phase mechanism limits phase boundary movement because of low mutual solubility and slow migration of charge carriers.

Solid solutions ranges σ and 1-β increase with reduction of particle size.

A. Yamada et al., 2001

# $LiFePO_4$: effect of nano-sizing and surface disordering

## XRD

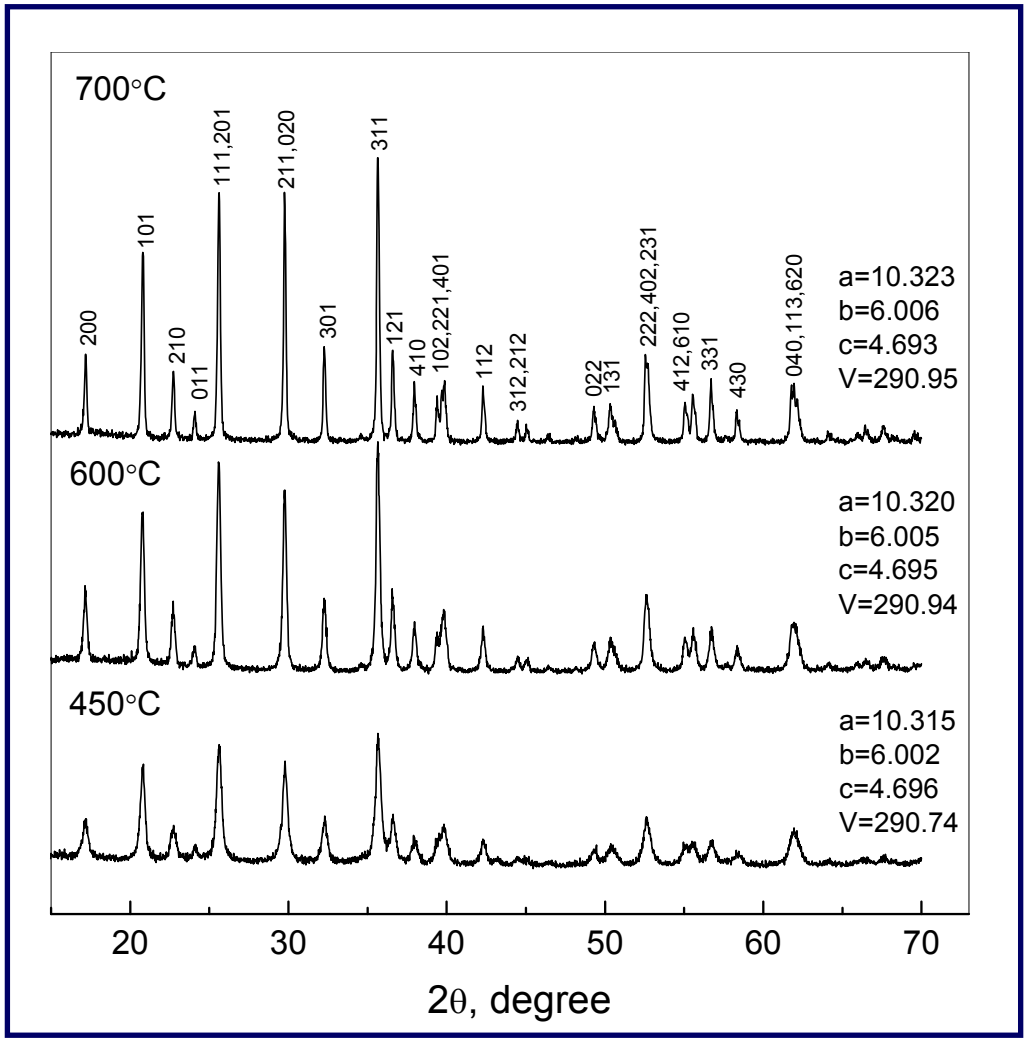


## Mössbauer spectroscopy

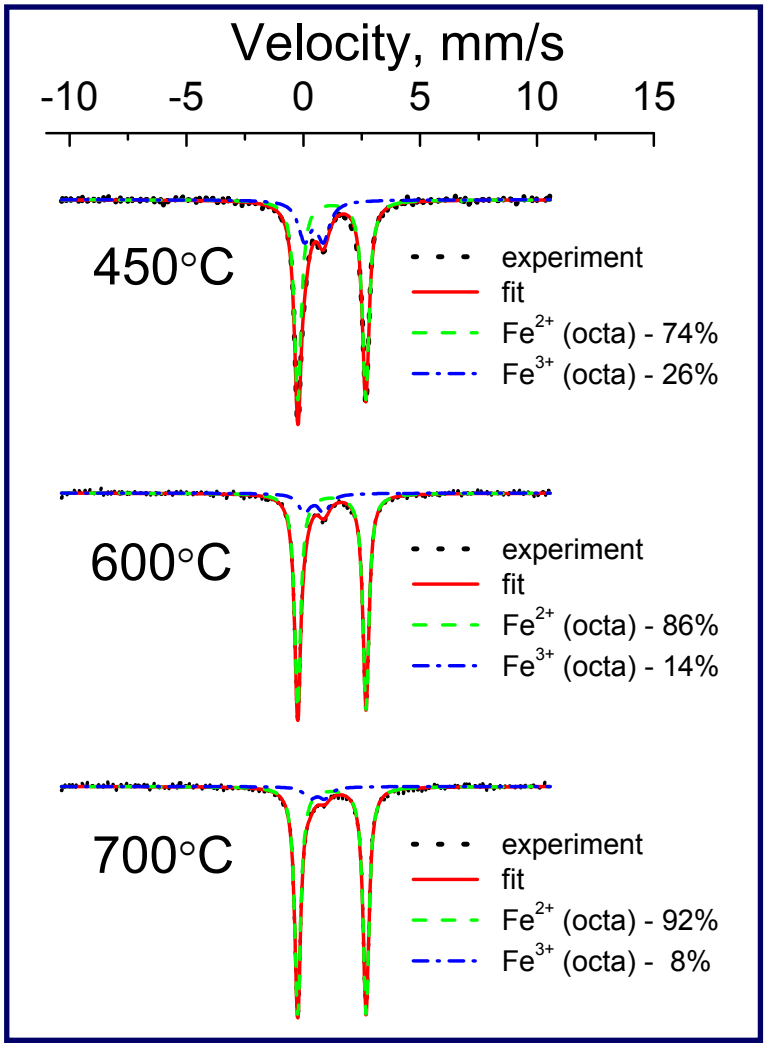




N.V. Kosova et al., 16 IMLB, Jeju, Korea, June 17-22, 2012.

# $LiFe_{1-y}Mn_yPO_4$ solid solutions

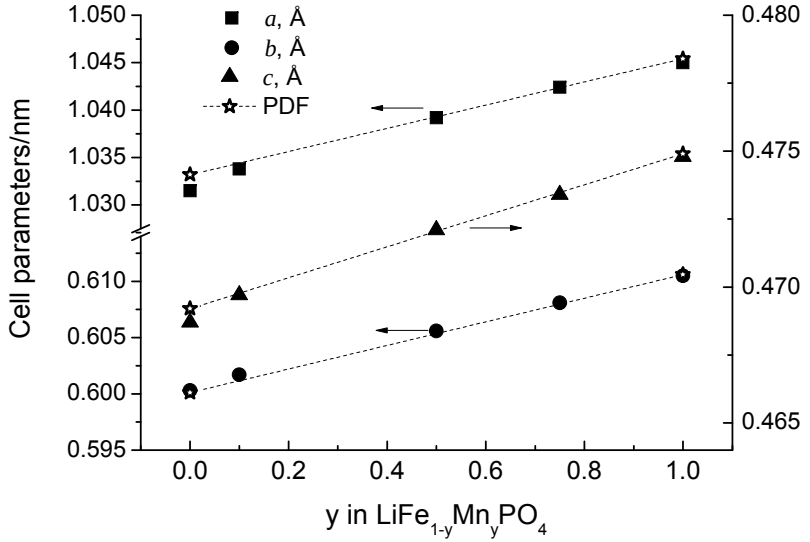


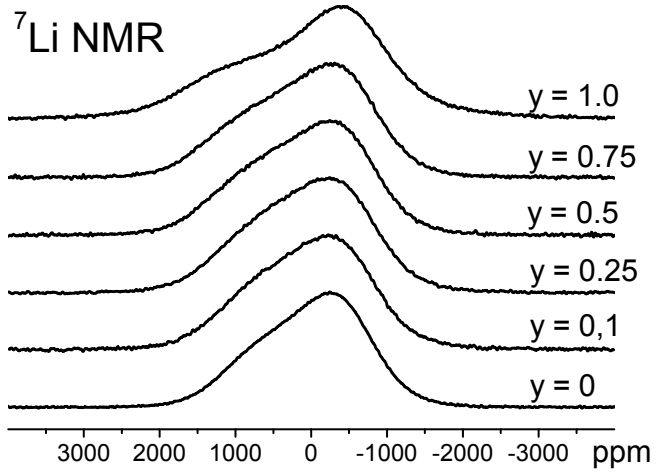


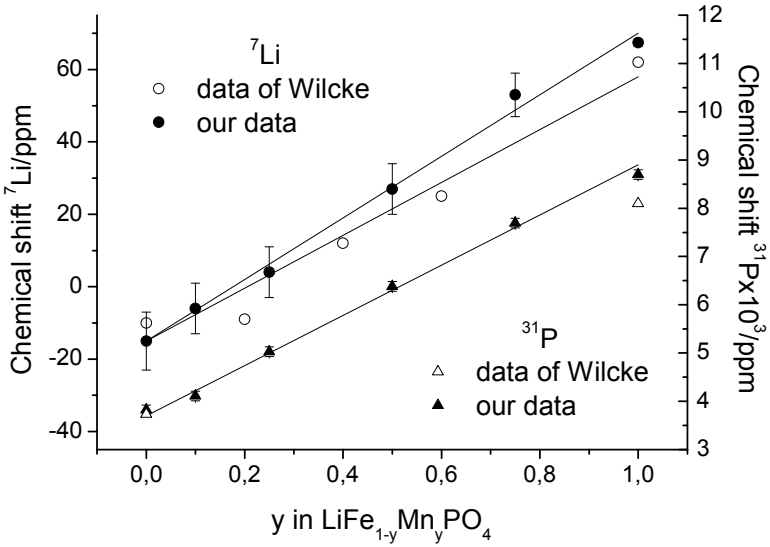


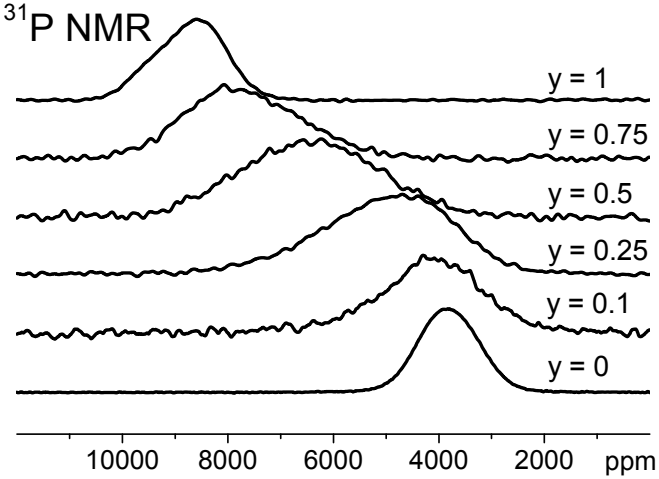




N.V. Kosova et al., Electrochim. Acta 59 (2012) 404-411.

# $LiFe_{1-y}Mn_yPO_4$: electrochemistry

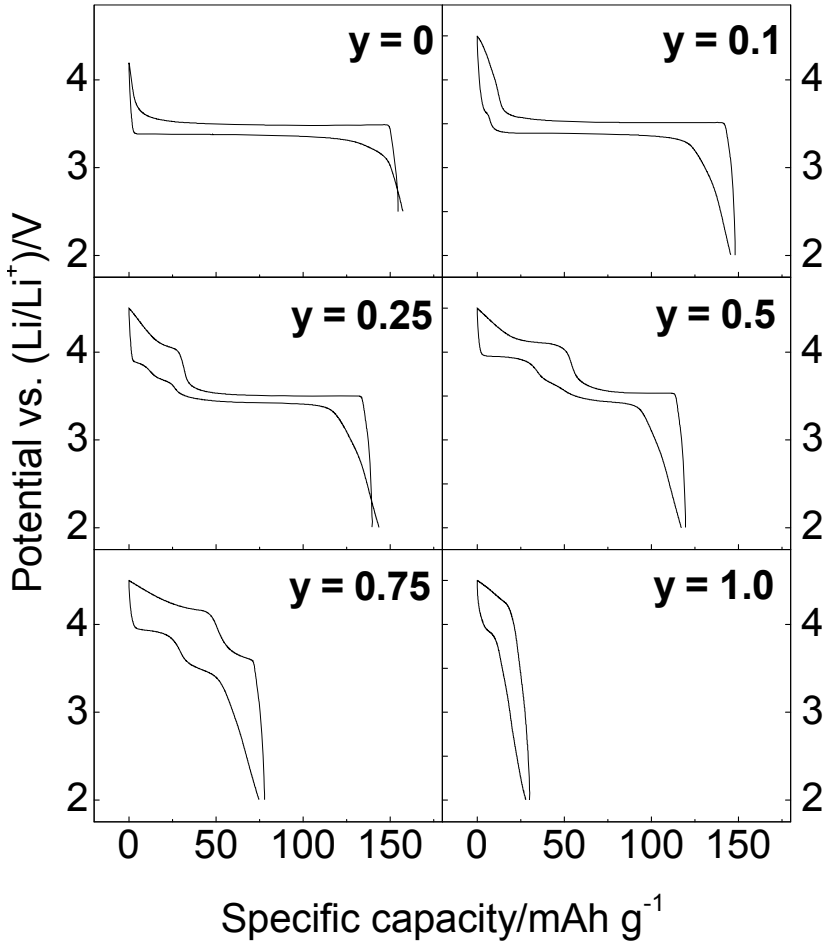


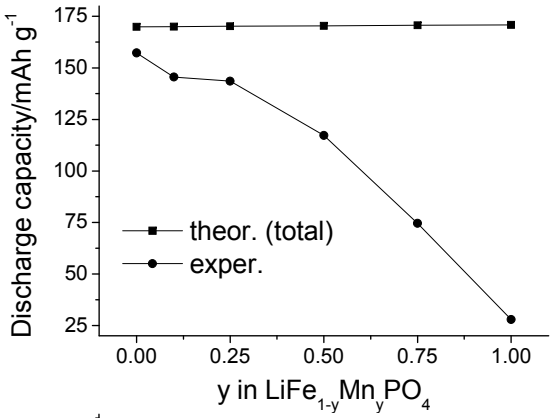


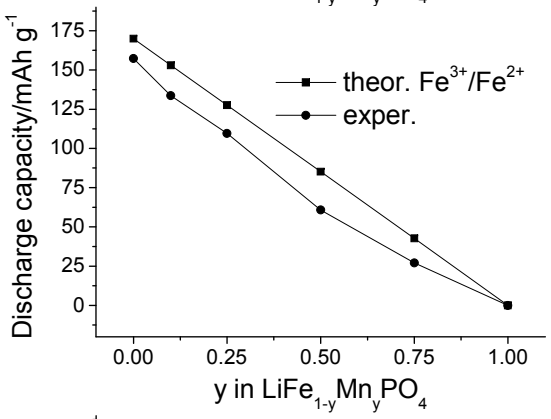


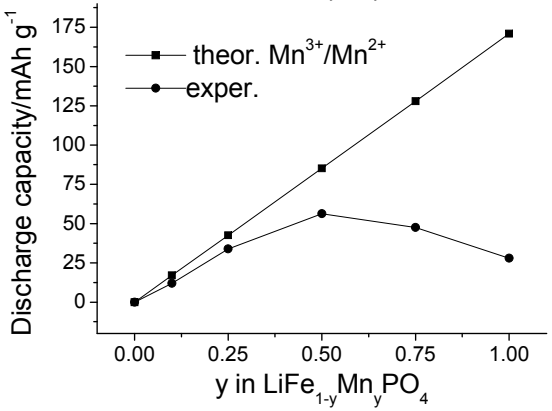

# *In situ* synchrotron diffraction study of $LiFe_{0.5}Mn_{0.5}PO_4$

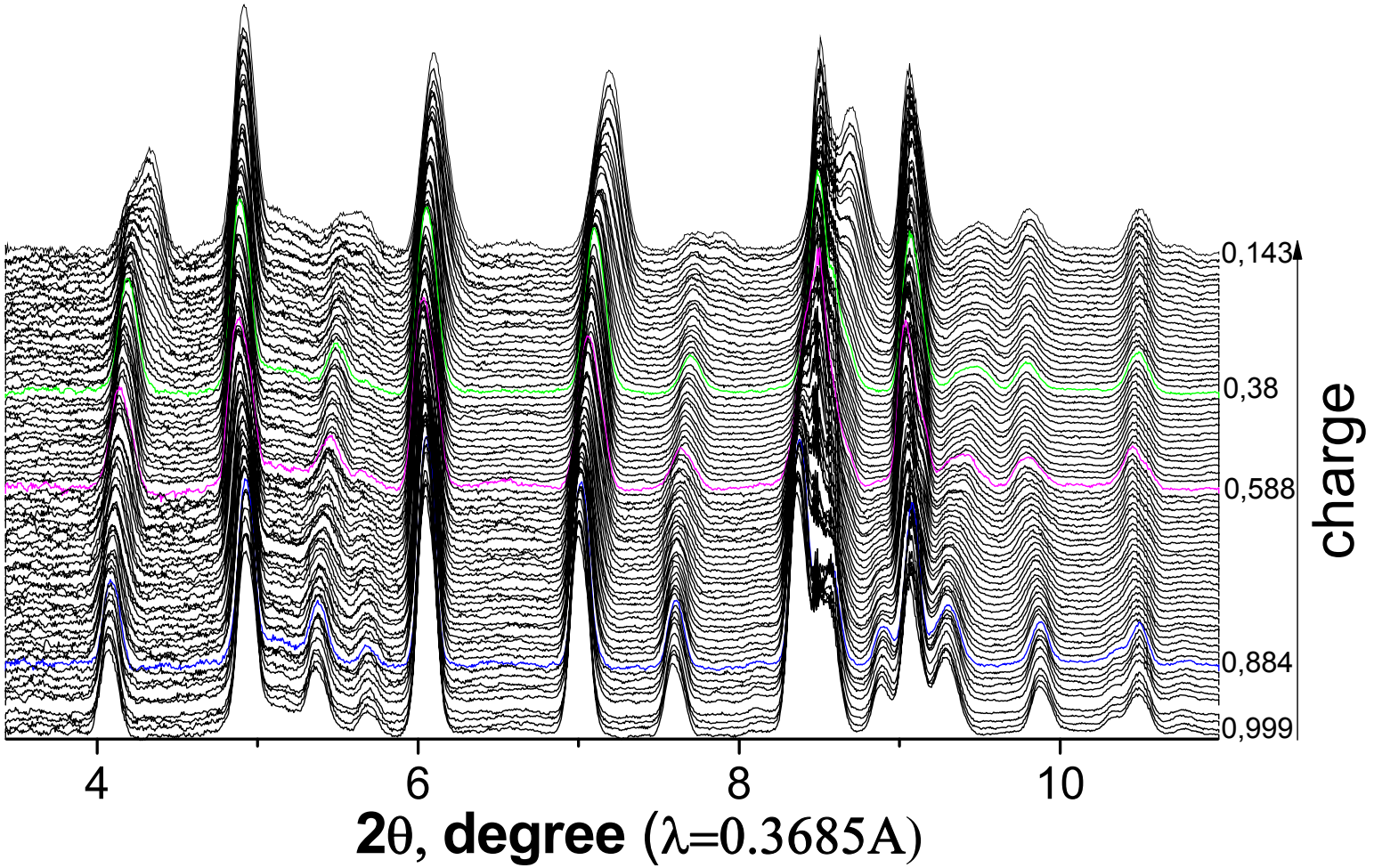


N.V. Kosova et al., Solid State Ionics doi:10.1016/j.ssi.2012.01.003

# *In situ* synchrotron diffraction study of $LiFe_{0.5}Mn_{0.5}PO_4$

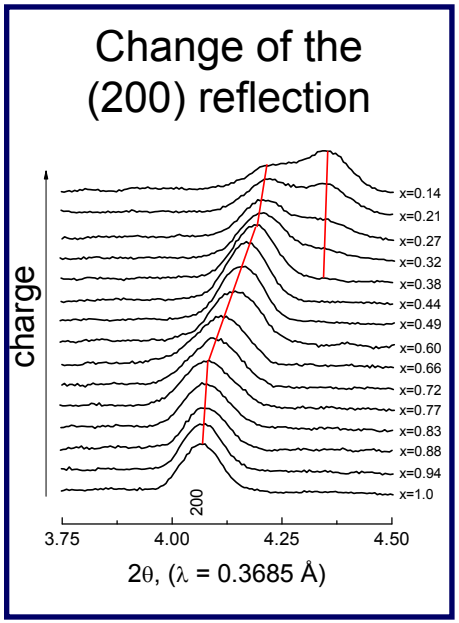


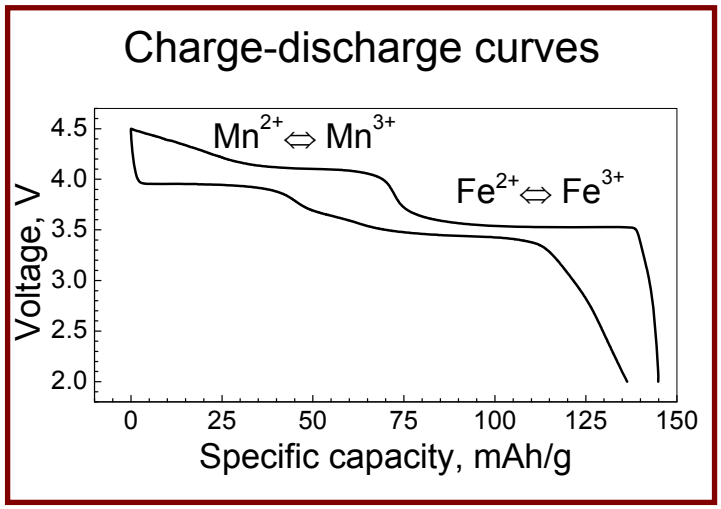


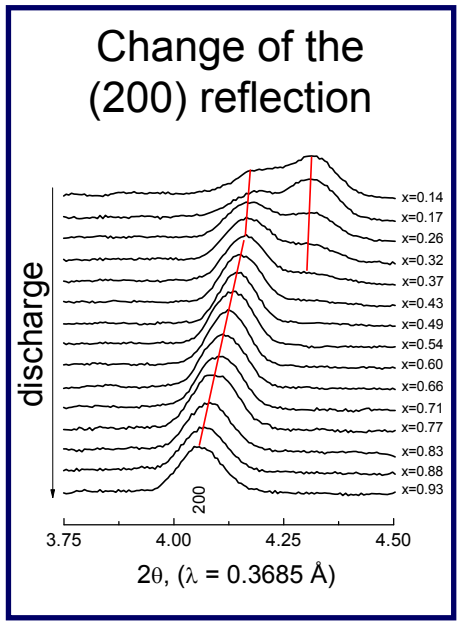


Cell parameters upon charge and discharge

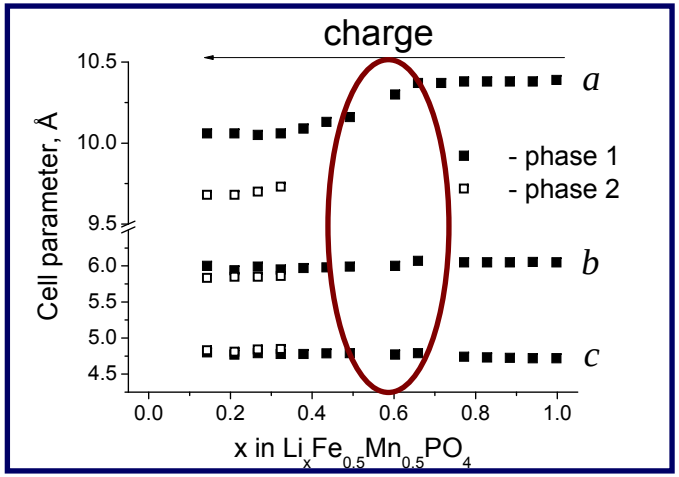


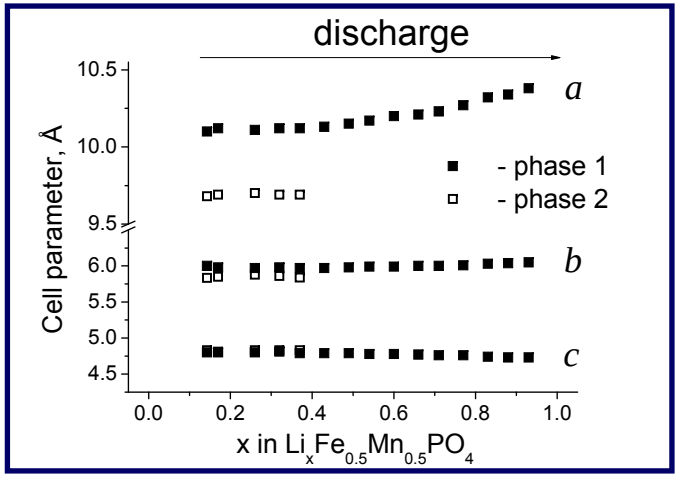


Wide intermediate range of single-phase reaction was revealed.

# $Li_{1.3}Al_{0.3}Ti_{1.7}(PO_4)_3$ (Nasicon) – solid electrolyte

Without MA

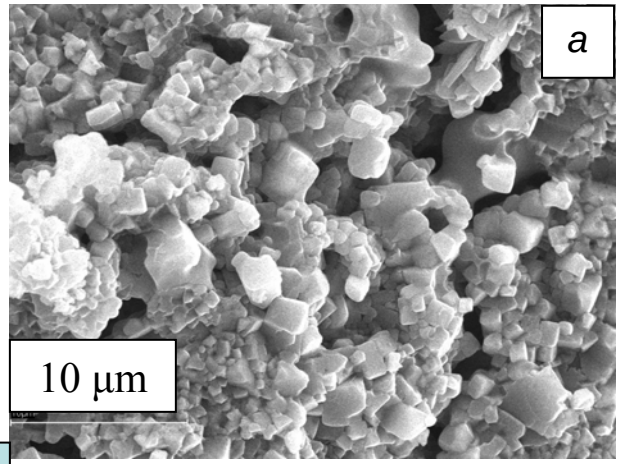


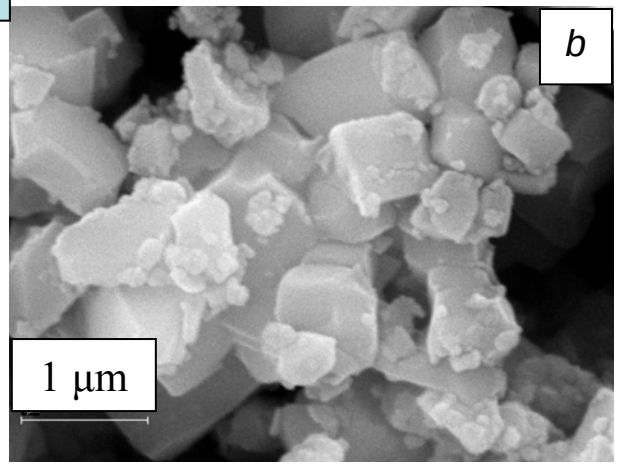


With MA

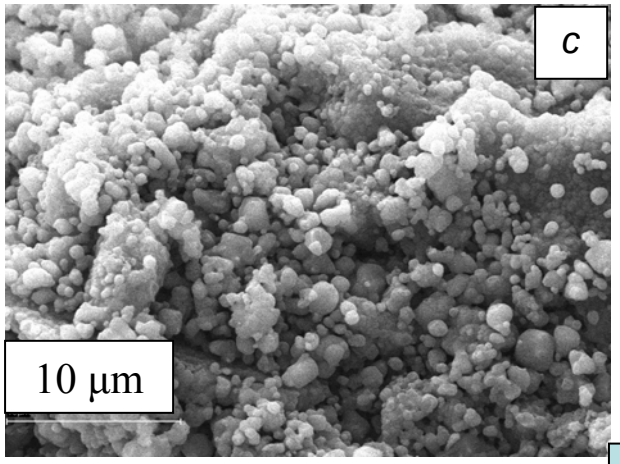


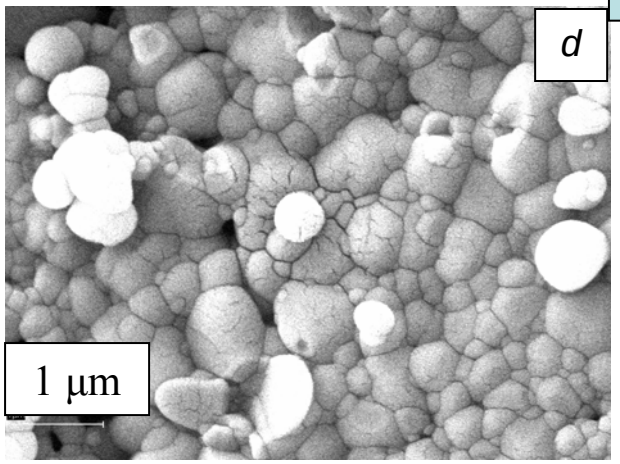


MA samples are characterized by:

1) lower particle size and larger particle size distribution;
2) rounded form of particles instead of cubic form for ceramic samples;
3) higher Li surface concentration.



N.V. Kosova et al., Ionics 14 (2008) 303-311.

# Ionic conductivity of LTP and LATP

LTP

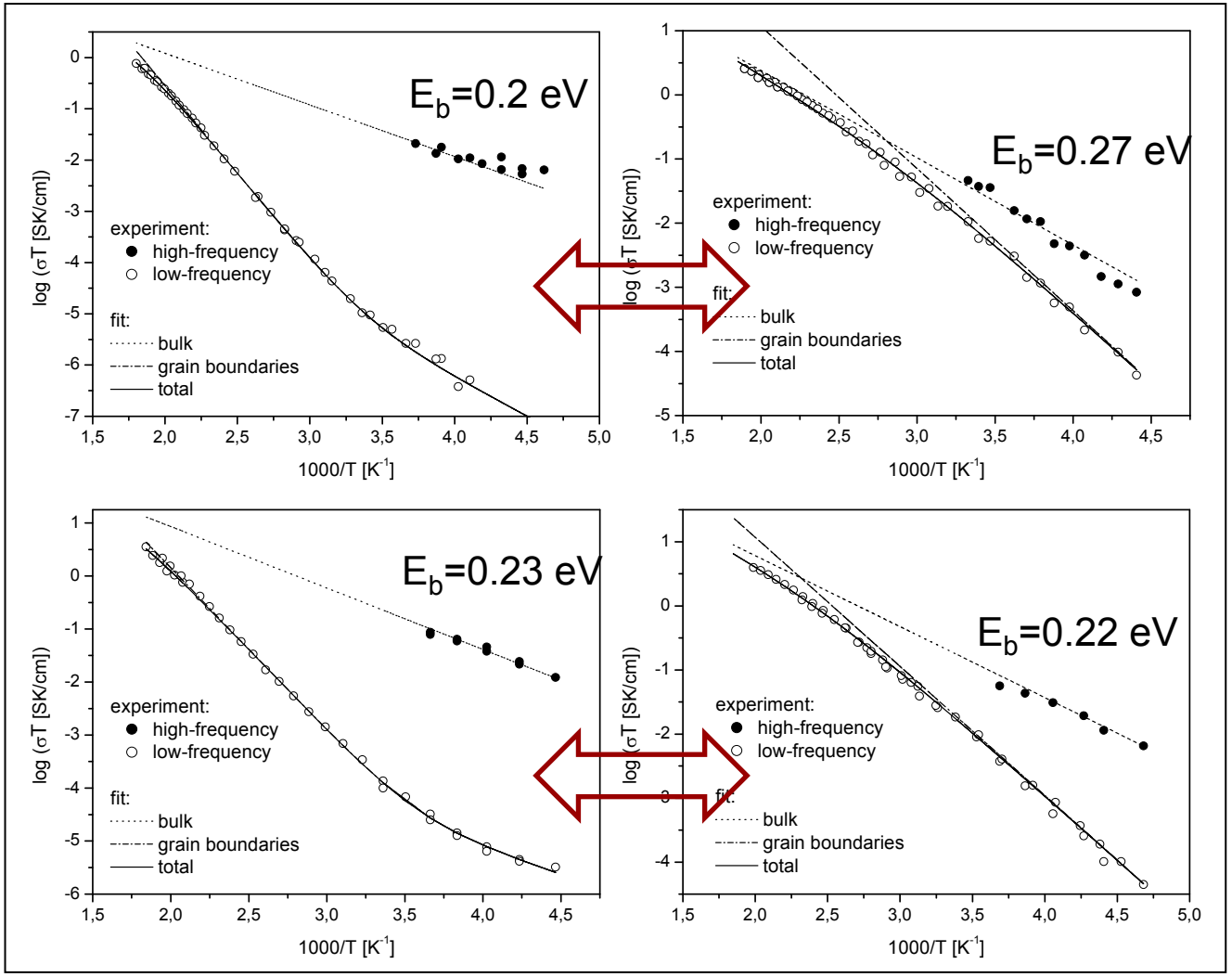


LTP-MA

$\sigma = 2 \cdot 10^{-5}$ S·cm$^{-1}$ at room T

LATP

LATP-MA

$\sigma = 6 \cdot 10^{-5}$ S·cm$^{-1}$ at room T

MA leads to a significant increase (by a factor of a thousand) in grain boundary conductivity of LTP and LATP.

# Nano-micro ‘core-shell’ materials

# Nano-micro ‘core-shell’ materials

capsulation (non-conductive coating)

modification (diffusion into the ‘core’)

composites (conductive coating)

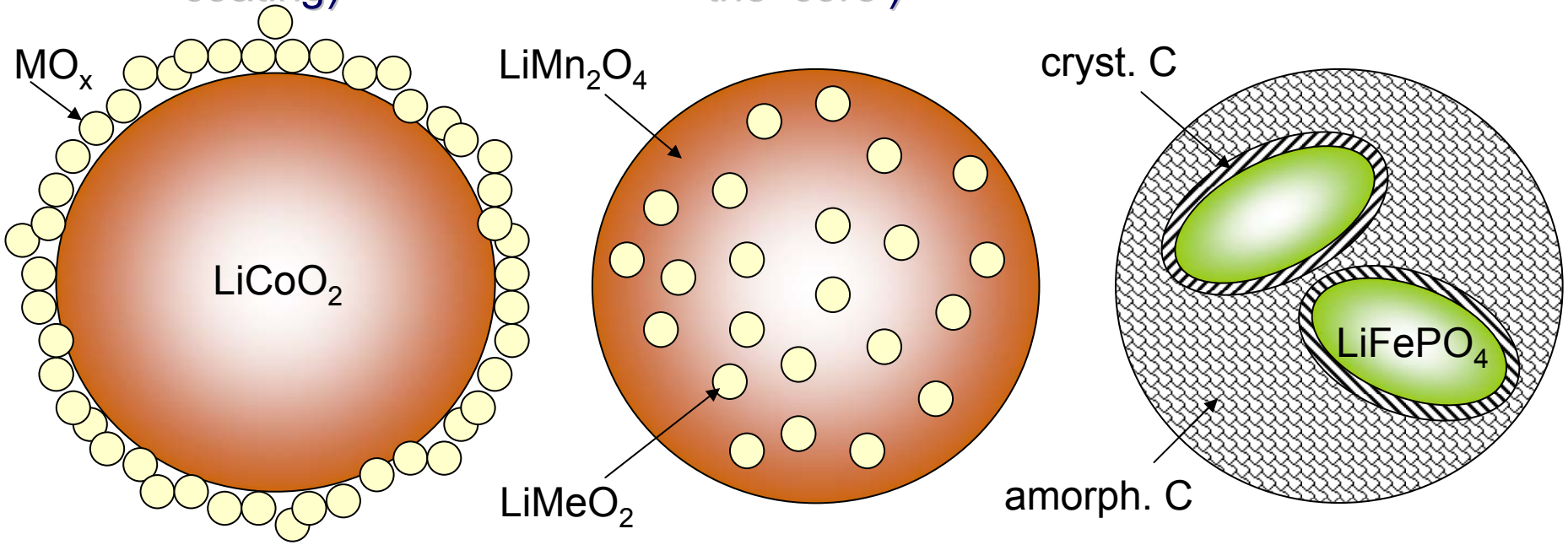


$LiCoO_2/MO_x$

Suppression of side reactions with electrolyte, improved stability to overcharge

$LiMn_2O_4/LiMeO_2$

Suppression of Mn dissolution in electrolyte, acceleration of electron-Li-ion transport

$LiFePO_4/C$

Increased electronic conductivity

# Surface modification of $LiCoO_2$ ($Al_2O_3$)

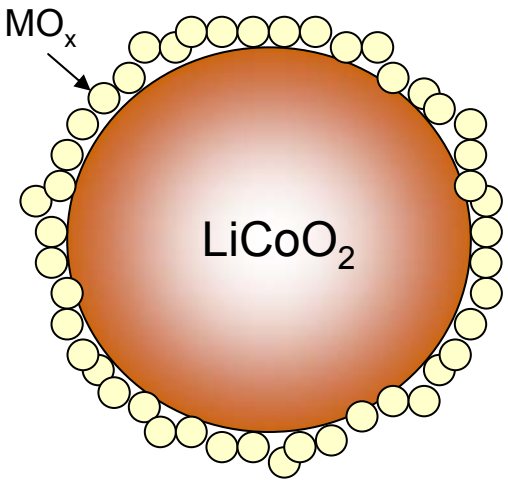


- non-conductive coating
- of small thickness (<50 nm)
- porous (permeable for electron and Li-ion transport)
- prevents side reactions with electrolyte
- improves stability to overcharge

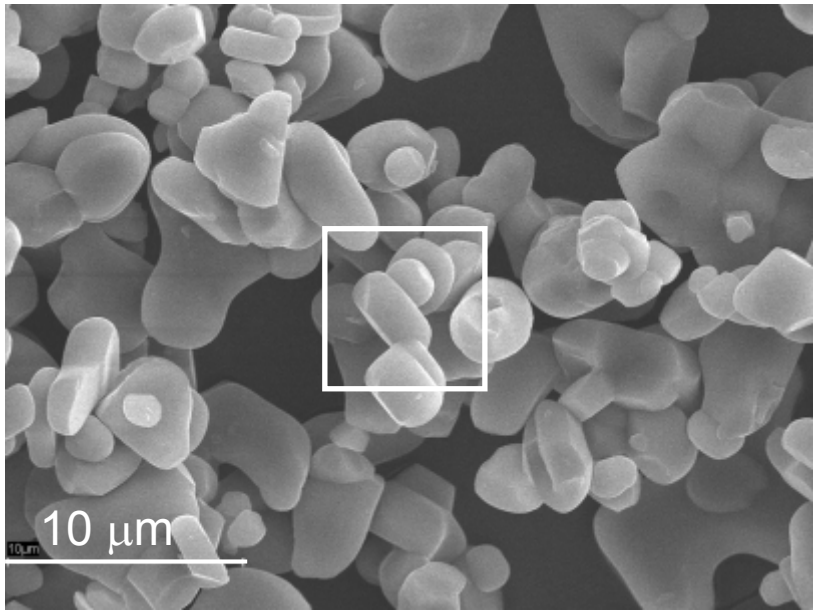


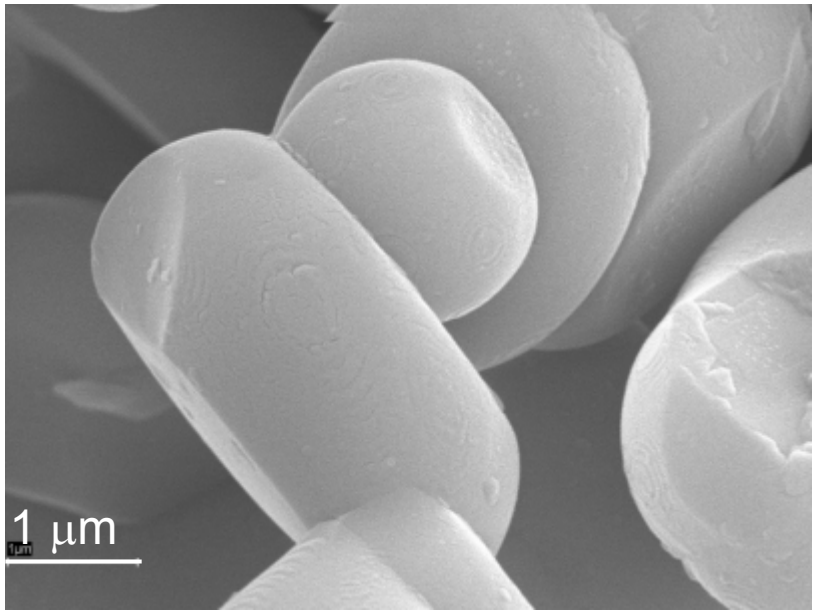


N. Kosova et al., Solid State Ionics 179 (2008) 1745-1749.

# Solution and MA surface modification approaches

Sol

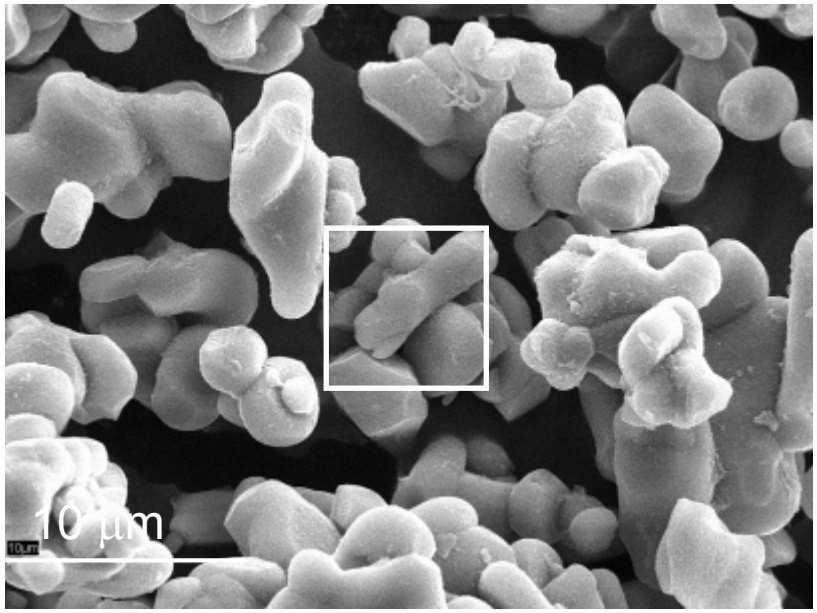


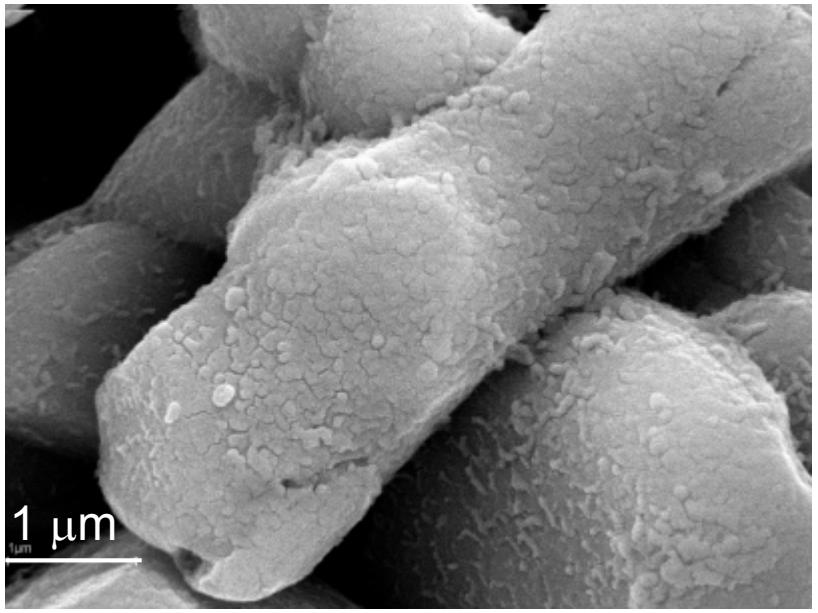


MA

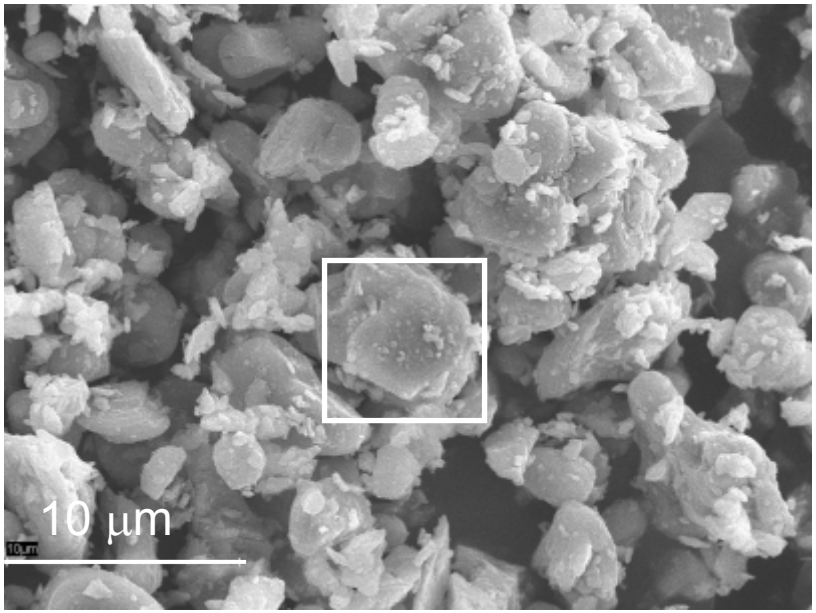


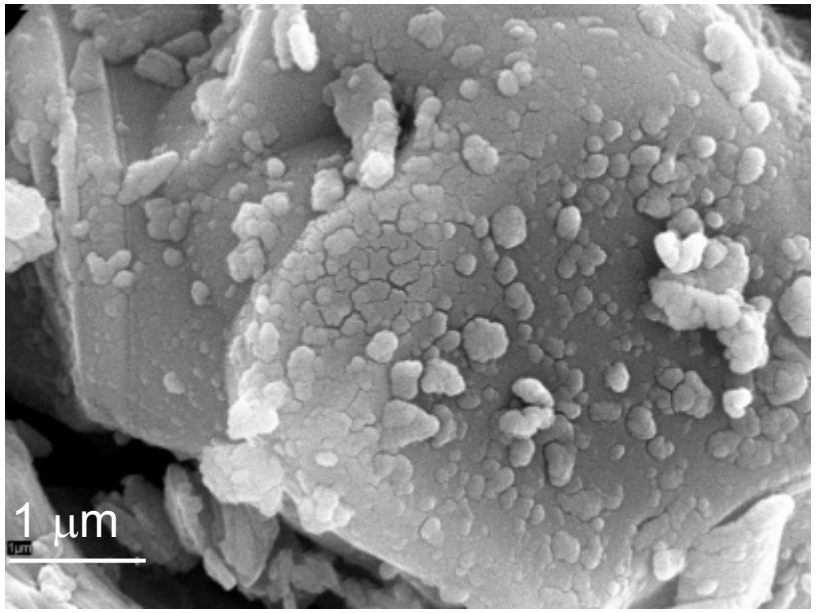

# Electrochemical performance of $LiCoO_2/MO_x$

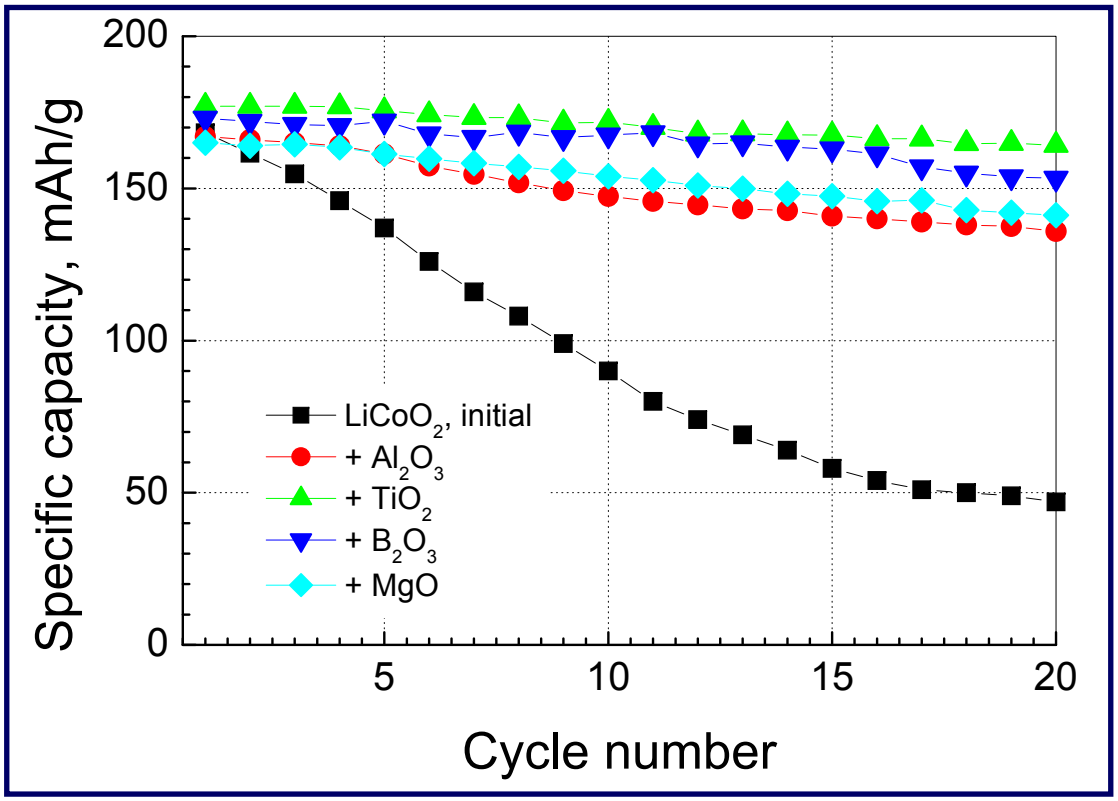


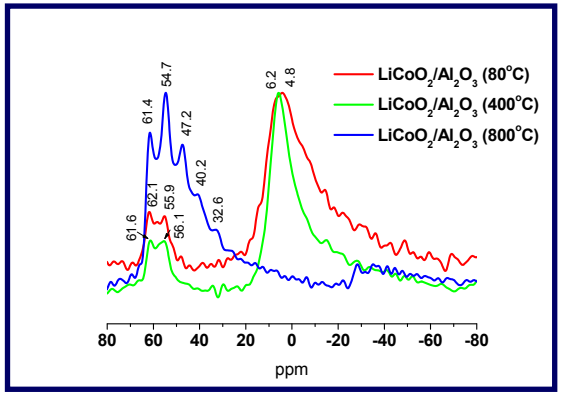


$^{27}Al$ MAS NMR of $LiCoO_2/Al_2O_3$

Increased discharge capacity due to a higher cut-off voltage (4.5 V) and improved cyclability

N.V. Kosova et al., J. Power Sources 174 (2007) 959-964.

# $LiMn_2O_4/LiMO_2$ (M: Co, Ni, $Ni_{0.8}Co_{0.2}$)

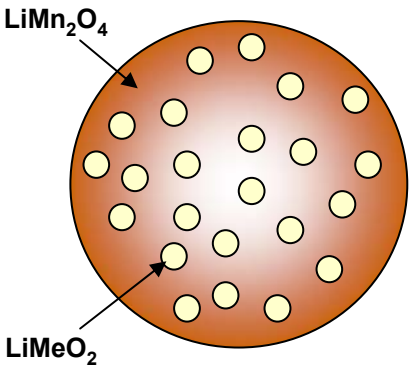


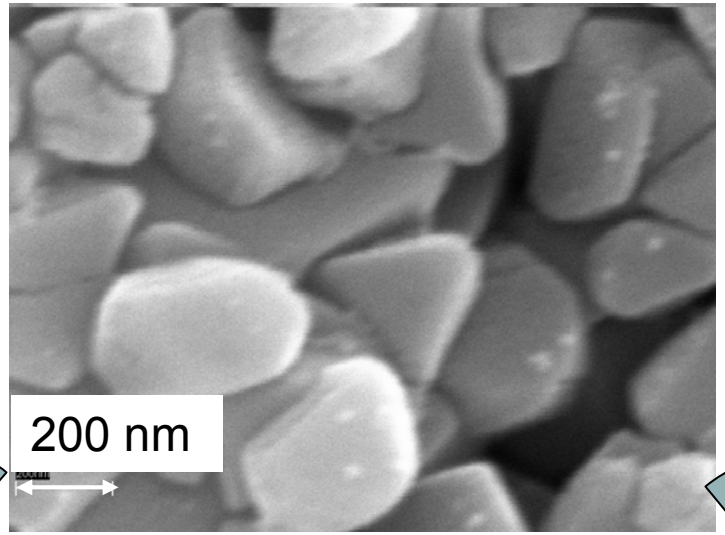


- conductive coating
- “reactive” coating
- suppresses Mn dissolution in electrolyte
- accelerates electron/ion transport at SEI

Initial $LiMn_2O_4$

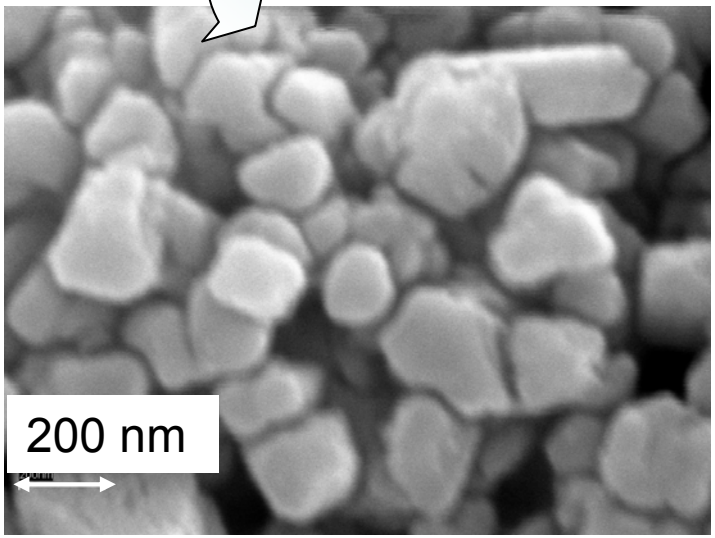


Solution method

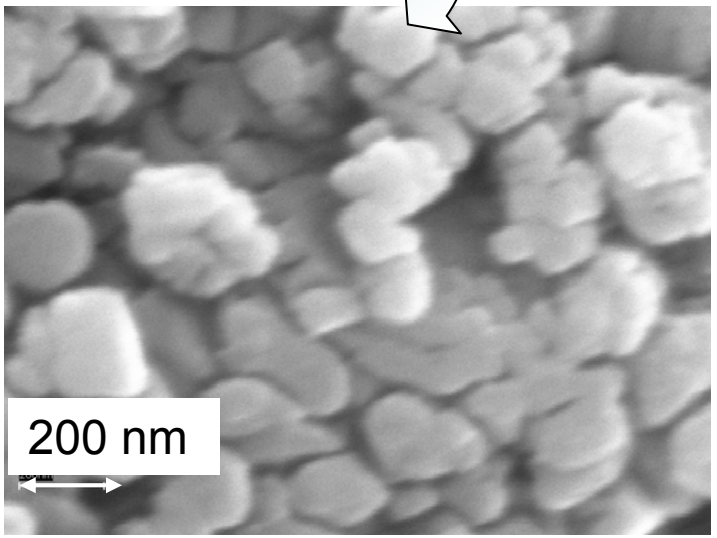


MA

# $LiMn_2O_4/LiMeO_2$: cycling

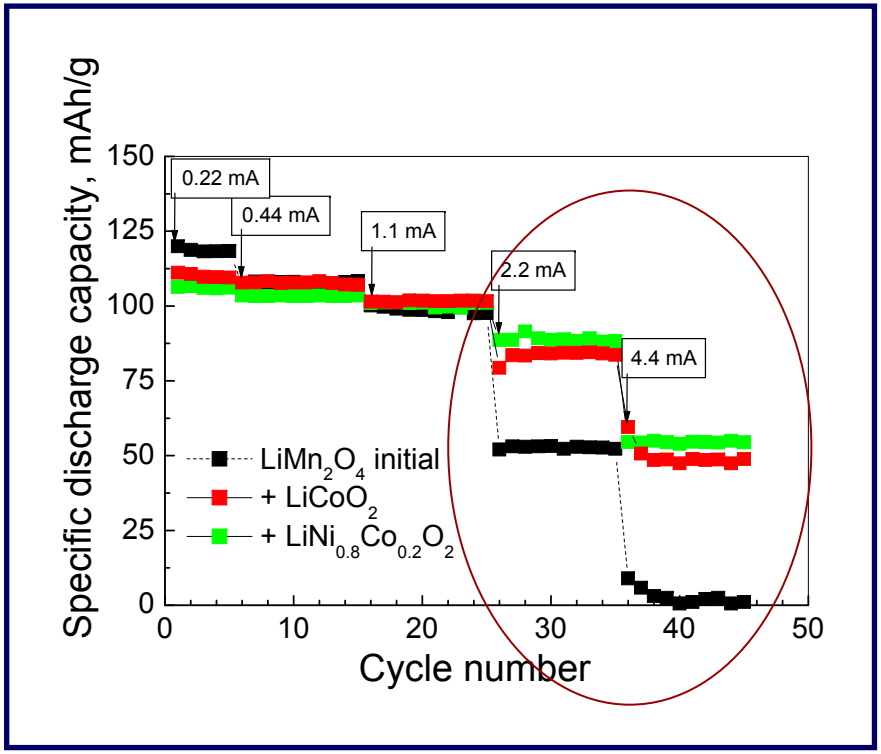


Improvement of high-rate performance

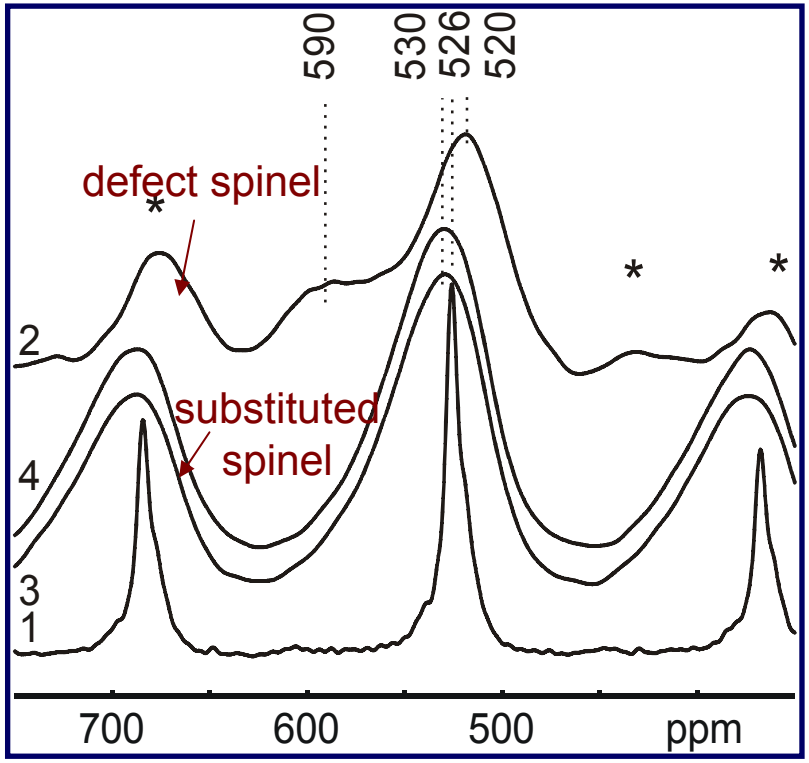


$^6Li$ MAS NMR of $LiMn_2O_4$, surface modified by $LiCoO_2$: *1* – bare, *2* – annealed at 400°C, *3* – 600°C, *4* – 750°C.

N.V. Kosova et al., Solid State Ionics 192 (2011) 284-288.

# XPS study of $LiMn_2O_4/LiMO_2$

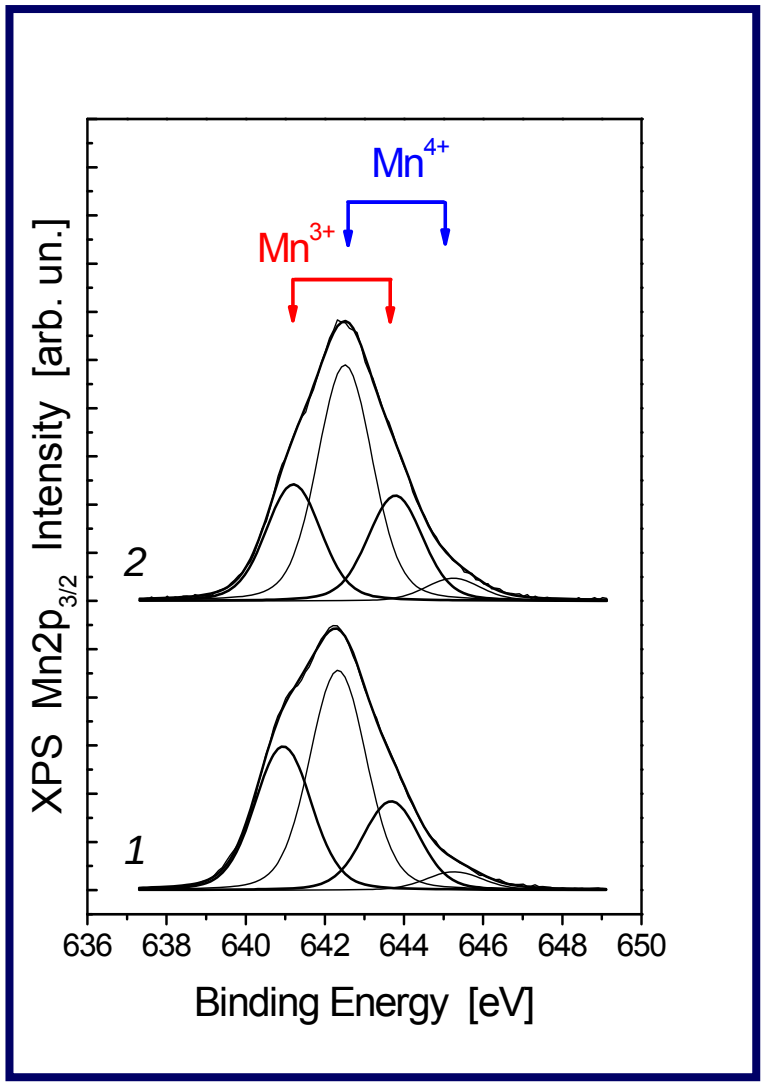


Mn$2p_{3/2}$ XPS spectra of pristine $LiMn_2O_4$ (*1*) and $LiMn_2O_4/LiCoO_2$ (*2*).

| Core/shell | Atomic ratio [Co]/[Mn] | Atomic ratio [Ni]/[Mn] |
|---|---|---|
| $LiMn_2O_4/LiCoO_2$ | 0.044/0.049* | - |
| $LiMn_2O_4/LiNi_{0.8}Co_{0.2}O_2$ | 0.020/0.021* | 0.016/0.024* |

* after Ar etching

'Shell' practically disappears after heat treatment of ground samples at 800°C due to the interaction with the 'core'.

In the case of $LiNi_{0.8}Co_{0.2}O_2$ coating, the surface concentration of Ni is lower than that of Co, probably due to accelerated diffusion of Ni ions into the bulk.

The surface concentration of $Mn^{3+}$ decreases.

# Composite (nanodomain) materials

# Composites $xLiMn_2O_4/(1-x)LiCoO_2$ (nanodomains)

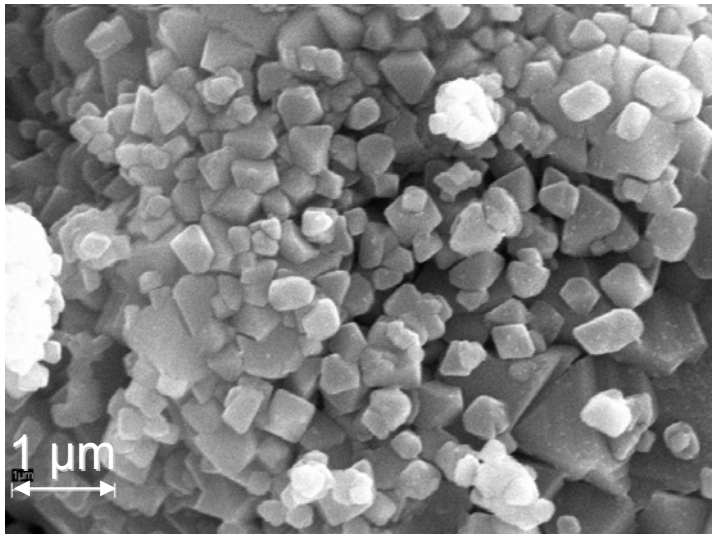


$LiMn_2O_4$

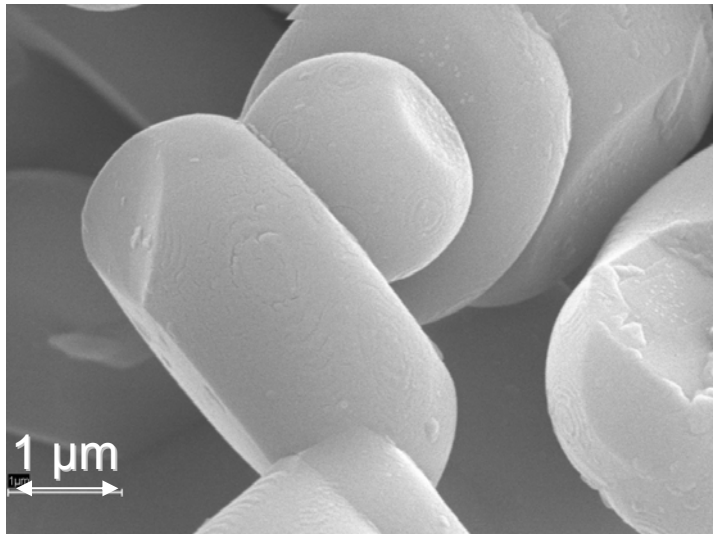


$LiCoO_2$

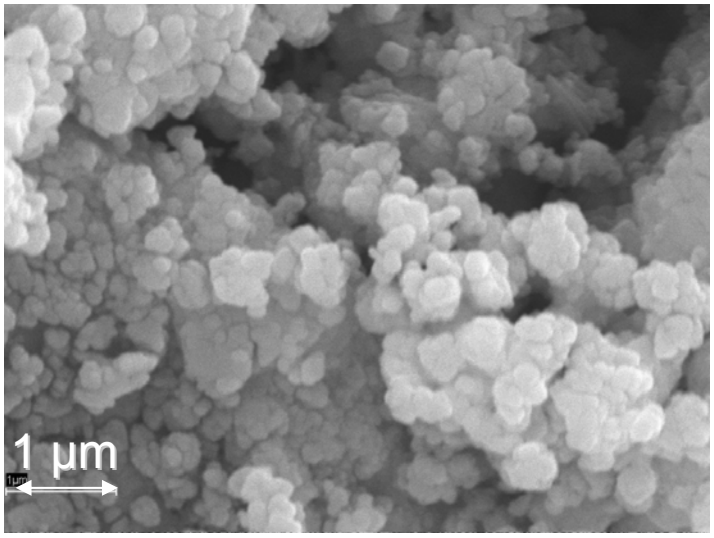


MA in high-energy planetary mill followed by heat treatment at 200-400°C

# Composites $xLiMn_2O_4/(1-x)LiCoO_2$: cycling

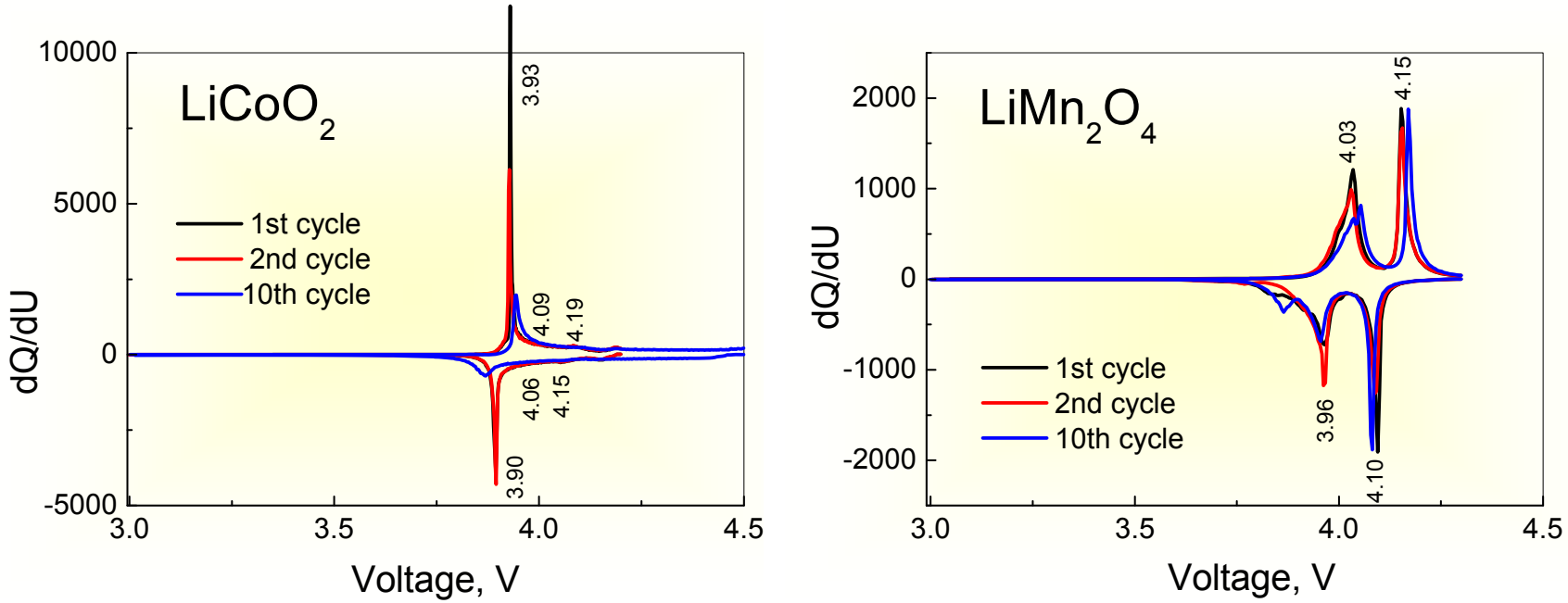


N.V. Kosova et al., Russ. J. of Electrochemistry 45 (2009) 277-285.

# Composites $xLiMn_2O_4/(1-x)LiCoO_2$: cycling

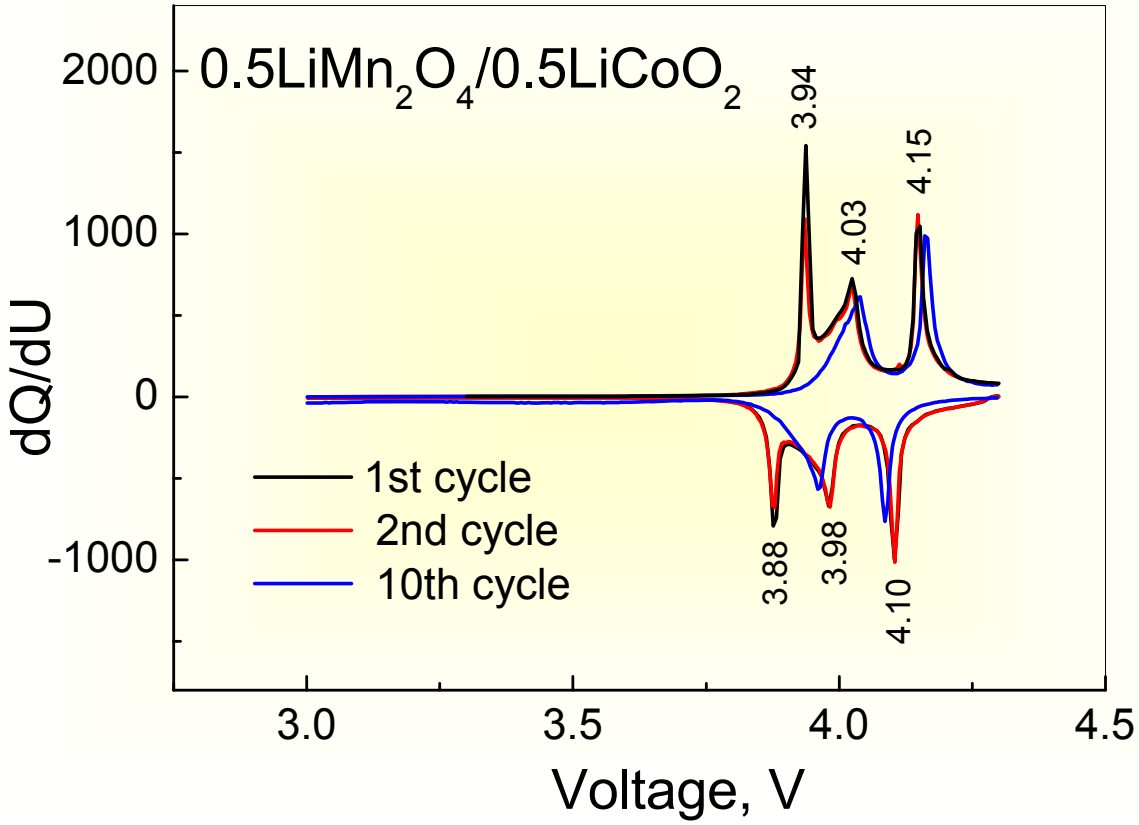


The redox peaks of $LiCoO_2$ gradually vanished during cycling indicating the occurrence of chemical interaction.

The composites are characterized by good capacity retention (100 mAh/g).

# Synthesis of the $LiFePO_4/Li_3V_2(PO_4)_3$ composites

**Method A:** (one-step) mechanochemically assisted combined CTR synthesis:

$$Li_2CO_3 + Fe_2O_3 + V_2O_5 + C + (NH_4)_2HPO_4 \rightarrow xLiFePO_4 / (1-x)Li_3V_2(PO_4)_3$$

**Method B:** (two-step) mechanochemically assisted mixing of two individual components:

$$xLiFePO_4 + (1-x)Li_3V_2(PO_4)_3 \rightarrow xLiFePO_4 / (1-x)Li_3V_2(PO_4)_3$$

N.V. Kosova et al., 63rd Annual Meetinf of ISE, Prague, August 19-24, 2012.

# $LiFePO_4/Li_3V_2(PO_4)_3$: cycling

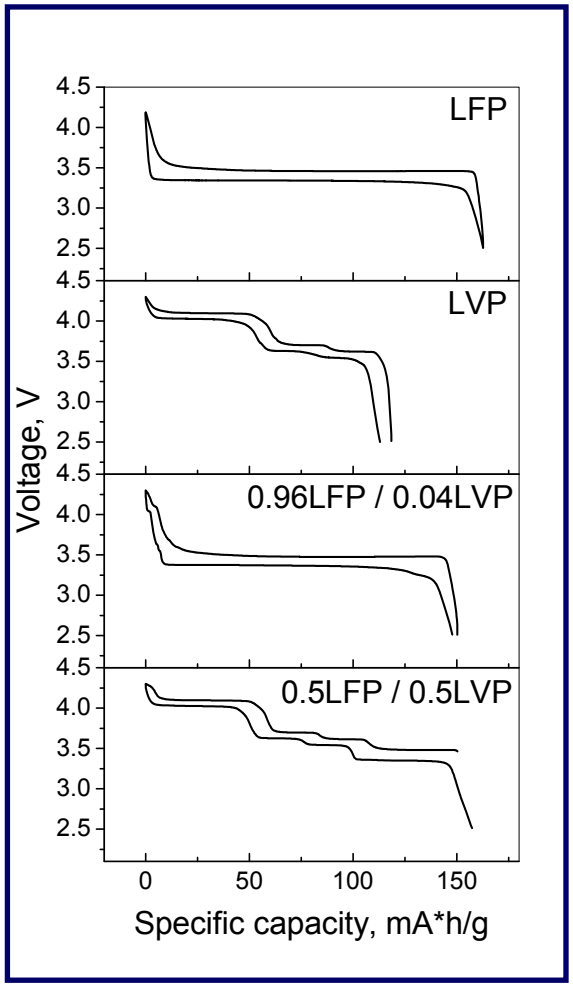


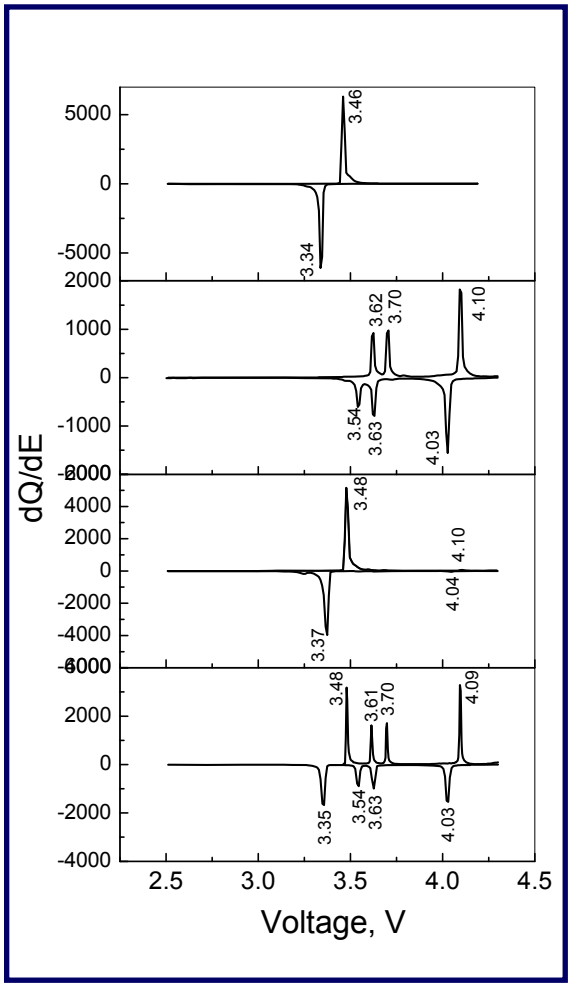


Some distinct plateaus are observed on the charge-discharge curves corresponding to two redox pairs: $Fe^{3+}/Fe^{2+}$ (at 3.4 V) and $V^{3+}/V^{4+}$ (above 3.4 V).

Low degree of polarization in the cycling curves shows that the electron and ion transport is facile.

As-prepared nanocomposites show excellent stability on cycling.

# Conclusions

- Mechanical activation using high-energy planetary mills is a promising solid-state method to prepare nanostructured electrode materials for Li-ion batteries
- Mechanical activation allows one to synthesize new composite ('core-shell', 'nano-domain') materials
- As prepared nanostructured materials differ from bulk materials by morphology, surface/bulk composition and electrochemical properties
- *In situ* synchrotron diffraction studies evidence the differences in the mechanism of lithium insertion/deinsertion upon cycling of nanostructured and bulk electrode materials

# Acknowledgements


- E.T. Devyatkina - XRD, cycling
- V.V. Kaichev - XPS
- A.T. Titov - SEM
- A.K. Gutakovsky - TEM
- A.B. Slobodyuk - NMR
- A.P. Stepanov, A.L. Buzlukov - NMR relaxation
- D.G. Kellermen - magnetic measurements
- S.A. Petrov - Mössbauer spectroscopy
- A.S. Ulikhin - impedance spectroscopy
- V.V. Ehler, A.V. Markov, V.K. Makukha - engineering

# Thank you for your attention!